Portland State University

PDXScholar

1987

A finite difference soil-structure interaction study of a section of the Bonneville Navigation Lock buttress diaphragm wall utilizing pressuremeter test results

Thomas C. McCormack
Portland State University

Follow this and additional works at: https://pdxscholar.library.pdx.edu/open_access_etds

🌀 Part of the Civil and Environmental Engineering Commons

Let us know how access to this document benefits you.

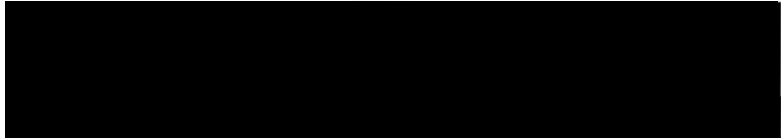AN ABSTRACT OF THE THESIS OF Thomas C. McCormack for the Master of Science in Civil Engineering presented on June 30, 1987.

Title: A Finite Difference Soil-Structure Interaction Study of a Section of the Bonneville Navigation Lock Buttress Diaphragm Wall Utilizing Pressuremeter Test Results.

APPROVED BY MEMBERS OF THE THESIS COMMITTEE:

Trevor D. Smith, Chairman

Franz N. Rad

M.M. Gorji

. Marvin H. Beeson

The P-y curve, used in current practice as an efficient line-load vs. soil displacement model for input into the finite difference method of laterally loaded pile analysis, is extended in this study for use with

cohesionless soils in diaphragm wall analysis on the Personal Computer with the BMCOL7 program. An analogous W-y curve is proposed, an elastic-plastic model with line-load limits developed from classical earth-pressure theories.

A new formula for predicting a horizontal wall modulus for cohesionless soils from the pressuremeter modulus is developed for use in predicting the displacements on the W-y curves. The resulting modulus values are shown to yield reasonable displacements values.

A new procedure for modeling preloaded tie-back anchors and staged excavation for diaphragm walls was developed, utilizing multiple computer runs, updated the W-y curves, and superposition of deflections.

These new developments were applied to a parametric study of a deflection-critical section of the new Bonneville Nav-Lock Buttress Diaphragm Wall, for which extensive high-quality pressuremeter test results were available. Deflection curves of the wall are presented, showing the effect of variations in anchor preload, wall cracking, anchor slip, at-rest pressure, and soil modulus.

The results indicate that preloading will reduce wall deflections by at least 4-fold, but that wall cracking can potentially double deflections. Safety factors against passive soil failure were determined to be about 5 at anchor preload, and more than 40 after full excavation.
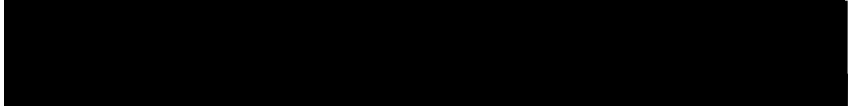
A FINITE DIFFERENCE SOIL-STRUCTURE INTERACTION STUDY

OF A SECTION OF THE BONNEVILLE NAVIGATION LOCK

BUTTRESS DIAPHRAGM WALL UTILIZING

PRESSUREMETER TEST RESULTS

by

THOMAS C. McCORMACK

A thesis submitted in partial fulfillment of the
requirements for the degree of
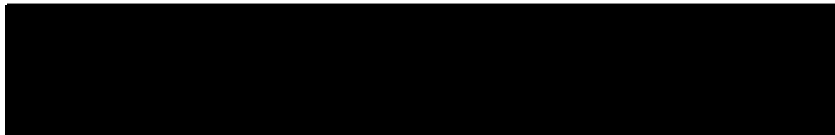
MASTER OF SCIENCE
in
CIVIL ENGINEERING

Portland State University
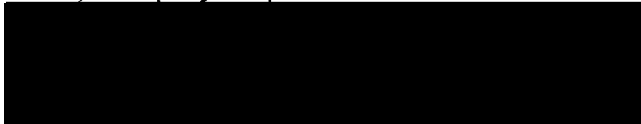
1987

TO THE OFFICE OF GRADUATE STUDIES AND RESEARCH:
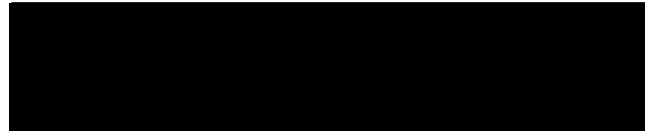
The members of the Committee approve the thesis of Thomas C. McCormack presented June 30, 1987.

Trevor D. Smith, Chairman

Franz N. Rad

M.M. Gorji

Marvin H. Beeson

APPROVED:

Franz N. Rad, Head, Department of Civil Engineering

Bernard Ross, Dean of Graduate Studies

DEDICATION

This thesis is dedicated to the author's wife, Susan K., and children, Joseph C. and Elizabeth J., whose love and support made the project both possible and worthwhile.

TABLE OF CONTENTS

LIST OF TABLES

LIST OF FIGURES

CHAPTER I

INTRODUCTION

THE NEW BONNEVILLE NAVIGATION LOCK

The U.S. Army Corps of Engineers (USACE), Portland District, is in the final design stage of a new Navigation Lock, related structures, and earthwork on the Oregon shore of the Columbia River at Bonneville Dam, 42-miles east of Portland.

Project Description

The existing Bonneville Project, which spans the river with features in both Oregon and Washington, consists of a spillway dam, 2 powerhouses, a navigation lock, and a fish hatchery.

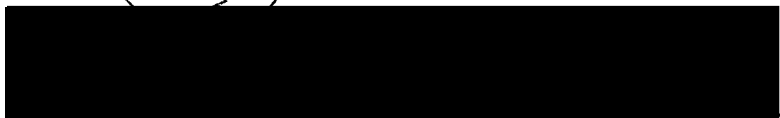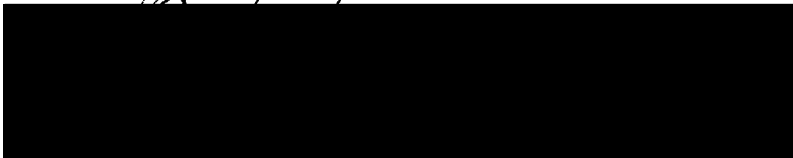The new lock will be located south of the existing lock on the Oregon shore, as shown in Fig. 1 (taken from the USACE Design Memorandum No. 3 (37)). The alignment requires relocation of the Union Pacific railroad that crosses part of the site. The main lock will consist of a massive gravity cast-in-place concrete structure, founded in a competent rock intrusion known as the Bonney Rock Intrusive. Downstream approach walls will be gravity mono-lith construction, founded in and retaining river deposits.
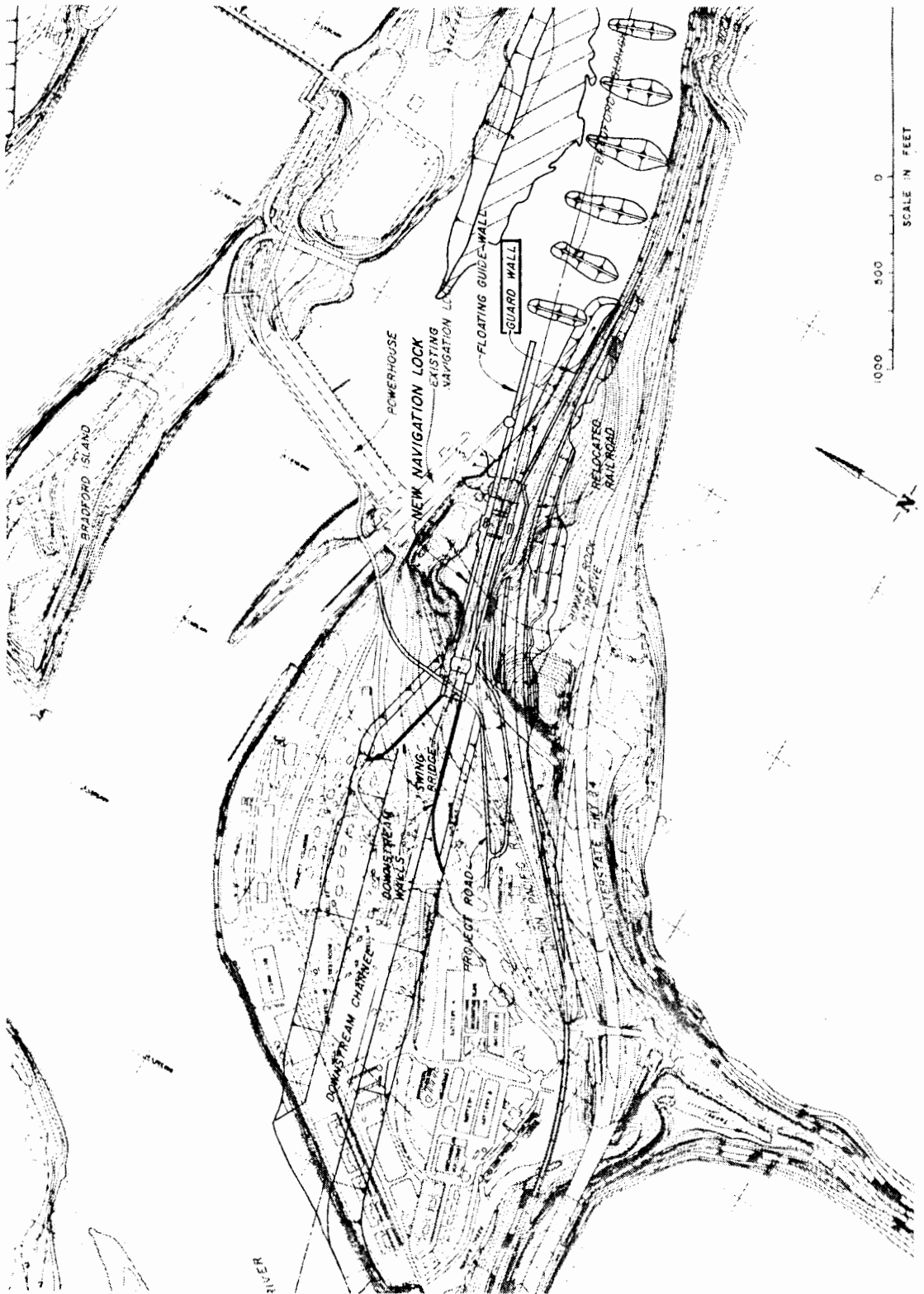
Figure 1. Vicinity Map, after USACE (37).

Upstream of the lock, a permanent anchored Buttress Diaphragm Wall (BDW), denoted as "Guard Wall" in Fig. 1, the topic of the present study, will be constructed in and retain Reworked Slide Debris (RSD) and Slide Block (SB) material. For the upstream 400-feet of lock structure, a temporary diaphragm wall is proposed to retain reworked slide debris encountered in that area during construction.

Local Geologic Setting

The temporary and the permanent buttress walls are located near the toe of the Tooth Rock Landslide (Fig. 2), a large Pliestocene age deep-seated slump block, which occurred 10,000 to 20,000 years ago in response to oversteepened slopes and high ground water levels caused by catastrophic flood waters from glacial Lake Missoula (37). Rapid movement of this slide during failure resulted in the mass sliding beyond the point of equilibrium. Although later episodes of Missoula flooding eroded much of the toe, the surface geomorphology indicates that the slide has been stable since the end of the floods, for at least 10,000 years. Most of the permanent buttress wall is embedded in, and retains, the Tooth Rock Landslide, which consists of two primary materials: large to massive displaced slide blocks (SB), and reworked slide debris (RSD).

In the vicinity of the wall, the SB material consists primarily of large intact rock blocks, ranging in size from
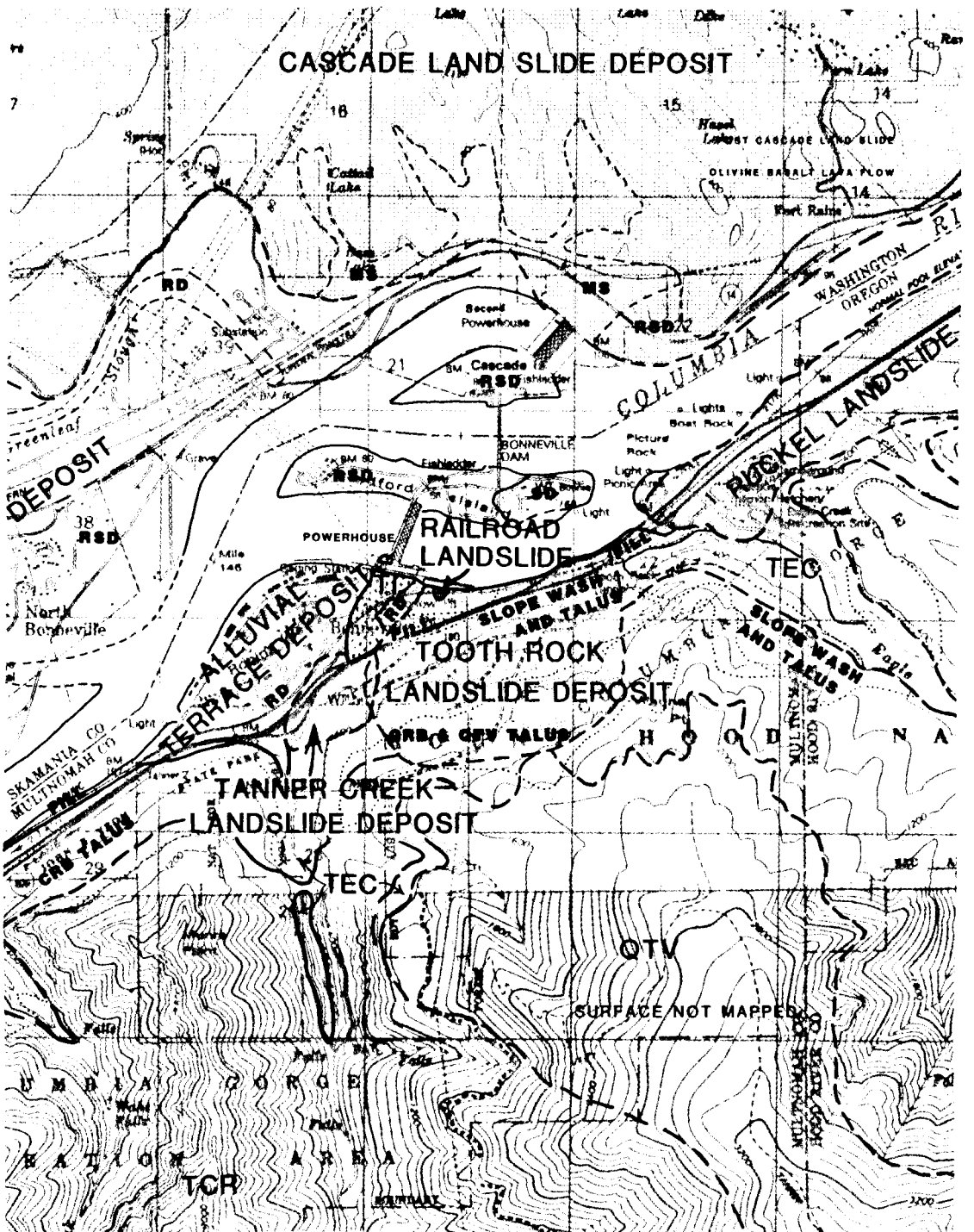
Figure 2. Surface Geology, after USACE (37).

tens to hundreds of feet, composed of Weigle Formation. The slide blocks are internally sheared and partially decomposed.

The RSD material consists of slide material that has been eroded and reworked by the Columbia River, resulting in a heterogeneous mixture of materials from silt to large boulders; much of the unit consists of hard angular rock fragments, with about 5-percent boulder-size to small slide block material. Recent age River Deposits locally overlie the RSD material at the ground surface.

Underlying the Tooth Rock Landslide materials, 2 in-place rock units exist: the Bonney Rock Intrusive (BRI) and the Tertiary age Weigle Formation (Tw).

The Weigle (Tw) unit in the project area consists primarily of fine-grained volcanic derived mudstone, siltstone, claystone, and local conglomerate lenses. The Tw is the oldest (upper Eocene) rock unit in the project area, and forms the foundation rock for the Bonneville Spillway Dam and Second Powerhouse. The unit is probably a lake or embayment deposit, which has undergone slight metamorphic alteration, imparting a greenish hue to the rocks. The beds of Tw strike N30E to N45E, & dip gently SE.

The BRI is a large, irregular diabase body that intruded the older Weigle and Eagle Creek Formations. Most of the BRI is west of the proposed wall location, where it acted as a resistant body and formed the western boundary

of the Tooth Rock Landslide. Smaller sills and plugs of
the BRI probably intrude the Weigle Formation, locally
altering the older rock.

Summary of Site Investigations

The following references pertain to site
investigation and analyses performed to date:

1) Geology, Excavation, and Foundation Design Memorandum
   No. 3, Bonneville Navigation Lock, USACE (37).

2) Pressuremeter Testing and Design Interim Report,
   Bonneville Navigation Lock, Smith (30).

3) Phase II, Tieback Test Program, Bonneville Navigation
   Lock, Squier (28).

4) Geotechnical Study: Exploration, Sampling, and
   Testing for Retaining Wall Parameters, New Bonneville
   Navigation Lock, Cornforth (6).

The present study seeks to apply high-quality
pressure vs. displacement information obtained from
extensive pressuremeter testing conducted at the Nav-Lock
site and reported in 2) above.

The Permanent Buttress Diaphragm Wall

The upstream approach will be bounded on the south
side by a 980-foot long permanent Buttress Diaphragm Wall
(BDW), the primary subject of this study, retaining
primarily landslide deposits, with a 30 to 50-foot dredge
depth. The embedded portion is 50-feet deep, to act as

seepage cutoff to enhance stability of the ancient Tooth-Rock Landslide.

The BDW will be installed using slurry trench construction techniques, and as designed consists of heavily reinforced concrete TEE sections, 13 to 14-feet deep. Tieback anchors will be installed at intervals through a grade-beam at the top of the wall. The ground surface retained by the wall will be called upon to support heavy equipment surcharge, and an embankment carrying the relocated double-track Union Pacific Railroad alignment.

The primary design criteria of the BDW is that railroad and navigation traffic not be disrupted, and the stability of the area be maintained during and after construction. The USACE desires that deflections nowhere on the wall exceed 1-inch, during and after construction.

SOIL-STRUCTURE INTERACTION

Limitations of Classical Design Methods

Traditionally, anchored bulkheads have been analyzed by assuming that the driving and resisting soil pressures are at the full active or passive limit condition, that a point of inflection exists either near the dredge line or not at all, and that the tie-back anchor undergoes negligible deflection. The anchor load, bending moment diagram, and embedment safety factor is then obtained by simple limit equilibrium statics.

These traditional procedures, when applied with judgement by experienced engineers, have proven adequate for flexible sheet-pile walls, whose flexural stiffness is generally small compared to the anchor and soil stiffnesses. However, the Bonneville BDW does not meet this criteria for traditional analysis techniques. The BDW is flexurally very stiff, and the 100 to 150-foot long tie-backs are well beyond the traditional lengths and are axially very flexible. Further, the traditional method does not permit a reliable method of calculating deflections, which are in the case of the BDW the primary design criteria. Clearly, some other technique must be employed to derive reliable design information.

The fundamental analytical problem is that both applied and resisting soil pressures vary depending upon wall movement, which in turn depends on those soil pressures, as well as on wall and anchor stiffness. A soil-structure interaction approach is required to analyze this highly indeterminate relationship.

The Finite Difference Method

Currently, the most efficient technique for solving soil-structure interaction problems is the Finite Difference Method (FDM), a 2-dimensional "beam on elastic foundation" analysis in which the differential equation of the elastic curve is discretized at nodes which react to

"Winkler Soil Springs". Matlock and Ingram (21) extended this method to include non-linear load-displacement expressions (p-y curves) at the nodes, and formulated a numerical solution, commonly known as the BMCOL Series; one of the earliest of the series is the BMCOL7 program (32).

The finite difference solution via BMCOL7 requires non-linear soil line-load vs. displacement information as input to the program, such as given by a typical W-y curve for walls shown in Fig. 3(b).

The Need for High Quality Soil Information

Lack of a soil line-load vs. displacement model of a precision consistent with a reinforced concrete or steel sheet-pile wall model, for input into BMCOL7, is a fundamental problem. Conventional field and laboratory testing methods emphasize limit (failure strength) parameters, are deficient in pressure vs. displacement information. Dissatisfaction with presently existing methods of estimating horizontal soil line-load vs. displacement is expressed in the literature (15).

Successful use of numerical solutions to soil-structure interaction problems mandates that the line-load vs. displacement information for the soil be of a quality comparable to that of the structural steel or reinforced concrete. At the present time, insitu pressuremeter testing has the highest potential for

providing usable information on the horizontal deformation of soil.

The Pressuremeter

The pressuremeter (PMT) was invented in France in the 1950's, and has a sound theoretical basis with over 30-years of practical application in France and elsewhere in the world.

The PMT consists of a cylindrical bladder which is lowered into a predrilled borehole and expanded by hydraulic or pneumatic pressure, as shown schematically in Fig. 3(a). The pressure required to inflate the probe (and hence the soil cavity), and the probe volume increase (and hence the radial strain of the cavity) are recorded and plotted, as shown on the right side of Fig. 3(a). The PMT can be mechanically visualized as an "inside-out" triaxial test, wherein the soil surrounding the insitu cavity is brought to failure by a measured principal stress state. It has enormous potential to increase our practical knowledge of the insitu behavior of soils from the information provided on the pressure vs. displacement relationship; this is apparant from the curve in Fig. 3(a), which is in fact a non-linear horizontal soil stress-strain relationship. Note it's similarity to a hypothetical non-linear W-y curve for a wall in Fig. 3(b).

An added feature of the PMT is the ability to obtain

pressure vs. displacement information in any situation wherein a borehole can be obtained. This is particularly significant in cohesionless materials, such as at Bonneville, from which it is almost impossible to obtain undisturbed soils for laboratory testing.

RESEARCH OBJECTIVE

The objective of this research was to study existing pressuremeter theories, and propose a new method for predicting W-y curves in cohesionless material to describe the line-load vs. displacement soil response for slurry-constructed retaining walls.

Secondly, a new procedure for modeling preloaded tie-back anchors for slurry-constructed walls was developed, for application with the W-y curves and BMCOL7 program.

Finally, these 2 new developments were applied to the BDW with the results of the pressuremeter tests conducted at the Bonneville Nav-Lock site by Smith (30). A parametric study of a critical section of the BDW was made to determine the effects of anchor preload, wall cracking, anchor slip, at-rest pressure, and horizontal soil modulus on deflections and bending moment.
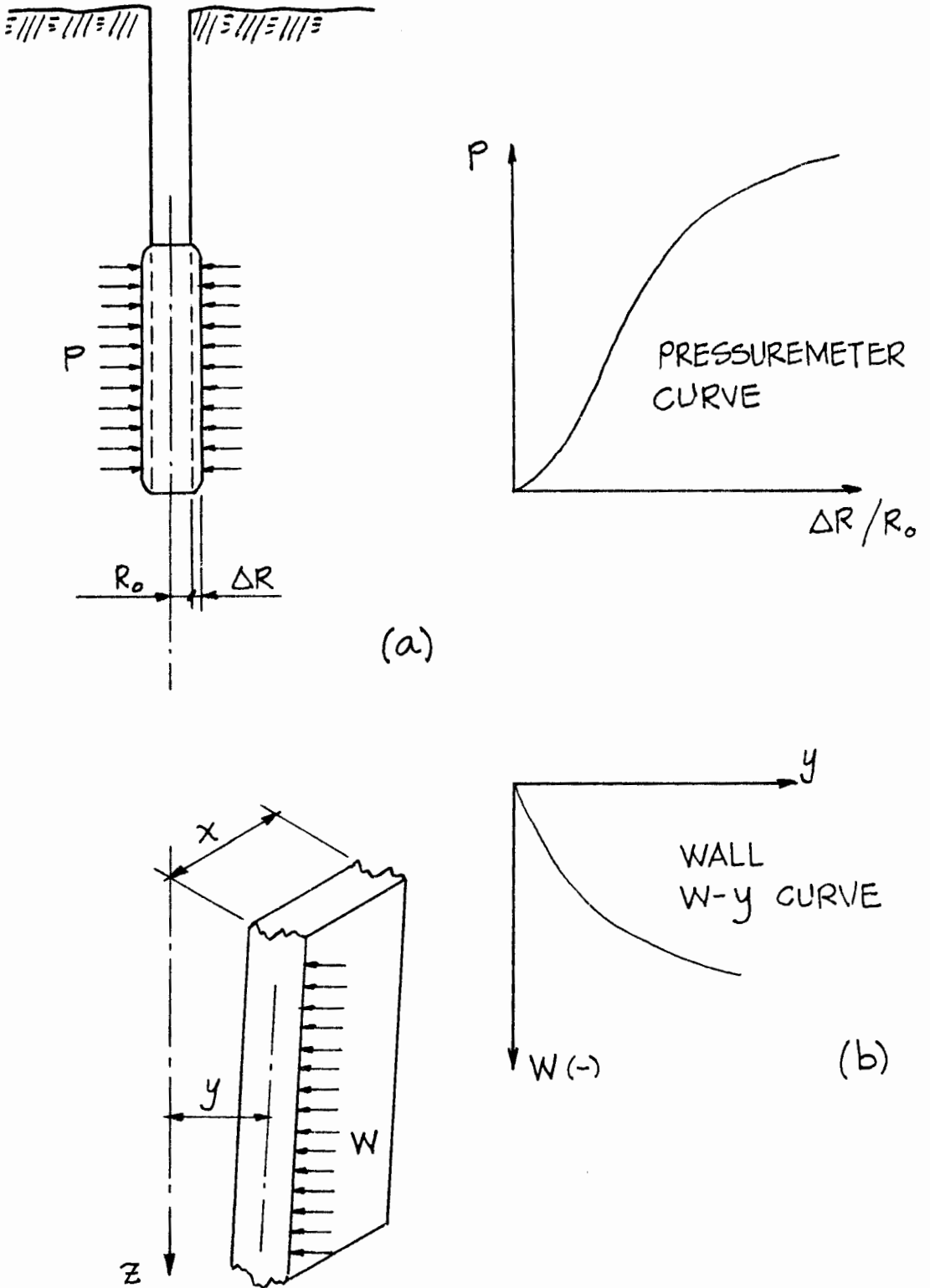
Figure 3. Comparison between pressuremeter p-ϵ_r and wall W-y curves.

CHAPTER II

SOIL-STRUCTURE INTERACTION FOR RETAINING WALLS

As stated in the Introduction, the correct solution
for displacements of a bulkhead retaining wall is a highly
indeterminate problem. The lateral flexural movement of the
wall must be compatible with the highly non-linear
horizontal stress-strain response of the soil in contact
with it.

THE FINITE DIFFERENCE METHOD (FDM)

Beam-on-Elastic-Subgrade Model

Currently, the most efficient method of solving the
soil-structure compatibility problem uses an extension of
the beam-on-elastic-subgrade model. The soil mass is
modeled as a series of discrete, closely spaced,
independent "Winkler" spring supports (after Winkler, who
in 1867 developed this idea to analyze railroad track).

Applying the beam-on-elastic-subgrade model to
vertical bulkhead wall analysis requires, obviously,
standing the beam "on-end", and a correct mathematical
formulation and solution to the problem which includes
non-linear Winkler soil springs.

Finite Difference Formulation

Based on the work of Hetenyi (13), the general differential equation for a beam/column-on-elastic-subgrade, with applied transverse loads, axial loads, and linear-elastic Winkler springs, is

$$EI \frac{d^4y}{dx^4} + P_x \frac{d^2y}{dx^2} = p - ky \qquad \ldots \ldots \ldots \ldots (1)$$

where

EI = Flexural stiffness of member (FL^{-1})

P_x = Axial compression (F)

y = Flexural deflection (L)

x = Distance along the member (L)

p = applied transverse line-load (FL^{-1})

k = Spring stiffness (FL^{-2})

Extension of Eq. 1 to the solution of soil-structure problems dates back almost 30-years, to research on the lateral load behavior of foundation piles on offshore structures, by Gleser (10), McClelland and Focht (20), and Matlock and Reese (18).

In the Finite Difference Method (FDM) (24), the flexural characteristics of the member and spring response of the soil is concentrated at each node. The model can be visualized as a linear structure made up of short, rigid members (the space between the nodes), each of which is connected by "flexible" joints (the nodes), to which may be

applied loads, rigid supports, or springs.

The governing differential equation, Eq. 1, is then approximated by a set of difference equations between the nodes. A non-linear soil response problem is solved by simultaneous solution of the difference equations, wherein repeated trial and adjustments to the soil spring stiffnesses are made until successive deflection solutions agree within an acceptable tolerance.

BMCOL7

The BMCOL series, a computerized finite difference solution of linear bending members with spring supports, began with Matlock and Ingram (21). The series was extended in the 1960's at the University of Texas/Austin, to incorporate non-linear springs and a variety of boundary conditions.

BMCOL7, a powerful and versatile design-oriented member of the BMCOL series, is currently available on both the Portland State University IBM Mainframe, as well an IBM-PC version in the Civil Engineering Department (39). The IBM-PC version of BMCOL7 was used in the analysis of the Buttress Diaphragm Walls for this study. The 100-foot high BDW was discretized into 100 nodes 1-foot apart. Relevant features of BMCOL 7 include:

1) Nonlinear loads, line-loads, and reactions can be freely discontinuous along the length of the

structure, input directly as p-y curves. The finite
difference solution is iterative, "updating" modulus
values between iterations as required to converge on
a compatible solution.

2) The program can model axial-flexural interaction.

3) Deflection or slope may be specified as boundary
    conditions at any node point.

4) Bending stiffness may be discontinuous and/or varied
    along the length of the member.

5) Nodal point tabulation and plot of net nodal force,
    deflection, slope, shear, and moment are produced.

6) The use of a recursion solution allows a rapid
    solution time to be achieved despite the necessary
    iterations. The current PC version in compiled BASIC
    generates a complete solution for a 100-node problem
    in less than 1-minute.

THE ELASTIC-PLASTIC W-y CURVE

As a retaining wall deflects laterally, the resulting
induced soil pressure or reaction varies with that
deflection. As described by Haliburton (14,15), the soil
response for bulkhead walls may be modeled at any point
along the height of the wall as a non-linear curve of
line-load vs. deflection, as shown in Figs. 4(c) and 4(e).
These curves are analogous to the the well-known "P-y"
curves used for the same purpose in modeling laterally

loaded piles. Haliburton further notes that simplification
of the curve to an "elastic-plastic" shape, as shown by the
dashed lines in Figs. 4(c) and 4(e), is reasonable, and
captures the relevant features of the soil response. The
elastic-plastic model will be followed for this study.

The At-Rest Intercept

A lateral (horizontal) soil pressure exists in an
undisturbed cohesionless soil deposit in which no movement
has occurred, and is referred to as the earth pressure
at-rest.

The ordinate at which the wall W-y curve crosses the
W-axis, shown as the W_O point in the left hand diagrams
of Figs. 4(b) and 4(d), represents the horizontal resultant
pressure on the wall corresponding to y = 0, i.e., no
movement, multiplied by the effective width (x dimension)
of wall under consideration. Since soils are generally
incapable of transmitting tension, pressures can act only
to push on one face or the other of the wall, and hence the
W-y curve is a plot of resultant horizontal line-load on
the wall. If the total vertical effective pressure in the
soil from all effects is the same on both sides of the
wall, W_O will be equal and opposite from each side and
the curve will pass through the origin of the W-y axes.
Typically, however, soil levels are different on opposite
sides, and W_O is shifted off the origin, as in Fig. 4.

18
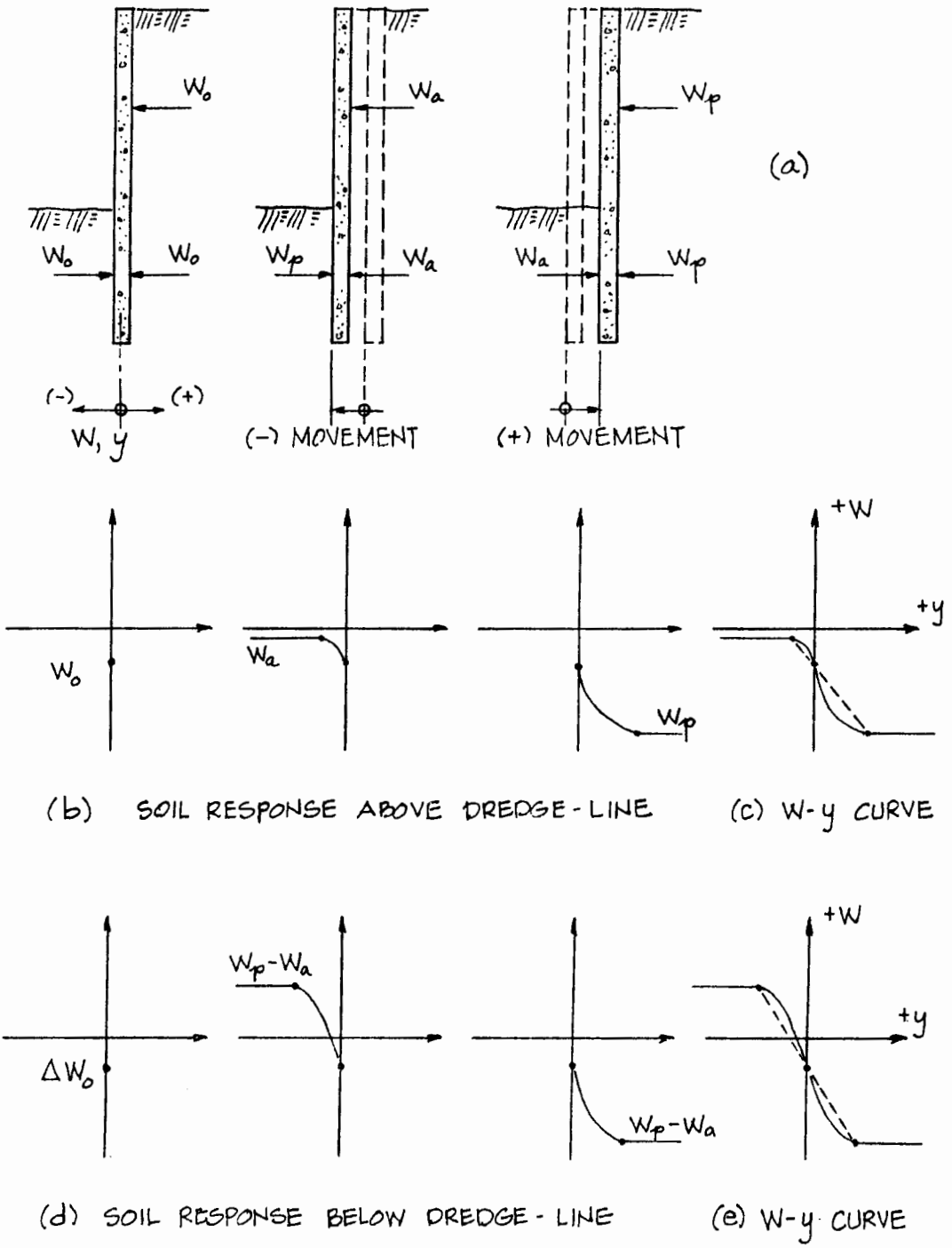
Figure 4. Elastic-plastic W-y curve derivation.

The at-rest intercept in a mass of undisturbed soil is computed by applying a coefficient, K_O, to the total vertical effective stress in the soil, multiplied by the effective wall width,

$$W_O = K_O \, \sigma'_V \, x \qquad \ldots \ldots \ldots \ldots \ldots \quad (2)$$

where W_O = horizontal at-rest line-load (FL^{-1})

K_O = coefficient of earth ressure at-rest

σ'_V = the total vertical effective stress at

the depth in question, including the effects

of surcharge loads

x = effective width of wall considered

The effective width of wall considered corresponds to the x-dimension shown in Fig. 3(b). For example, if a 15-foot wide TEE-section of wall is considered as the effective width, x is 15-feet. Alternatively, the structural section properties (EI, A) may be divided by 15, and x becomes 1-foot (the procedure used in this study).

The at-rest coefficient, K_O, is dependent upon the properties of the material, and the manner in which it was deposited. Establishing K_O precisely is not possible; a range of values can be estimated using engineering judgement and knowledge of the soil conditions likely to exist at the site. For sand, Terzaghi (35) gives a range of K_O from 0.4 to 1.2. The lower value is for sand deposited in horizontal layers without compaction.

K_o in ancient landslide deposits will likely be greater than 1.0, generated as part of the mechanism to stop the slide.

The Active and Passive Limits

Following the elastic-plastic W-y curve model, the sign convention is by definition the same for both W and y, and is generally (+) inward, toward the retained soil, and (-) outward, toward the channel.

From the middle figures in Figs. 4(a) and (b), it is apparant that for the fully excavated condition above the dredge line, (-) movement, i.e., to the left, at a given depth, will cause the at-rest line-load W_o, to decrease to a (-) active line-load, W_a. Movement to the right (+), as in the right-hand diagrams of the same Figs., will cause the at-rest line-load to increase to the (-) passive level available at that depth, W_p. Above the dredge line, both the active and passive line-loads are negative, since in each case the pressure is exerted outward against the wall. Fig. 4(c) gives a complete description of the soil response at a point above the dredge line.

Since the W value of the curve is actually the resultant of pressure applied to both sides of the wall, the value of the passive limit for a curve below the dredge line can be derived similarly, as shown in Fig.

4(d). For large (-) movements, the ultimate (+) line-load
is equal to the value of the passive line-load available
from the soil mass in front of the "toe", at the level for
which the curve is being drawn, minus the active value from
the retained side, i.e., W_p - W_a. Similarly, for
large (+) movements, the resulting (-) line-load is equal
to the passive value of the retained soil mass, minus the
active value exerted by the soil in front of the toe.

The value of the active and passive limits may be
obtained by applying a coefficient of active or passive
earth pressure, respectively, to the total vertical
effective stress in the soil at the depth in question,
multiplied by the effective wall width, as follows:

$$W_a = K_a \ \sigma'_v \ x \quad \ldots \ldots \ldots \ldots \ldots \quad (3)$$

$$W_p = K_p \ \sigma'_v \ x \quad \ldots \ldots \ldots \ldots \ldots \quad (4)$$

where W_a = active line-load at the depth in question

W_p = passive line-load available at that depth

K_a = the coefficient of active earth pressure

K_p = the coefficient of passive earth pressure

The value of the active and passive coefficents,
K_a and K_p, are available from classical limit
equilibrium theory. For cohesionless materials against
rough walls, the Coulomb Theory, dating from 1776, is still
applicable. From Terzaghi (34),

$$Ka = \frac{\sin^2(\alpha+\phi)}{\sin^2\alpha \ \sin(\alpha-\partial)\left[1+\sqrt{\dfrac{\sin(\phi+\partial)\ \sin(\phi-\beta)}{\sin(\alpha-\partial)\ \sin(\alpha+\beta)}}\right]^2}$$

$$\ldots \ldots \ldots \ldots (5)$$

and,

$$Kp = \frac{\sin^2(\alpha-\phi)}{\sin^2\alpha \ \sin(\alpha+\partial)\left[1-\sqrt{\dfrac{\sin(\phi+\partial)\ \sin(\phi+\beta)}{\sin(\alpha+\partial)\ \sin(\alpha+\beta)}}\right]^2}$$

$$\ldots \ldots \ldots \ldots (6)$$

where α = Angle of wall back face from vertical.

β = Angle of sloping surcharge above horizontal.

∂ = Angle of wall friction.

ϕ = Angle of internal friction of the soil.

The Horizontal Modulus

In the preceding discussion, it was shown that the ordinate values for the W-y curve can be established, or estimated, from classical soil mechanics. Less information is available to estimate the amount of displacement from at-rest to produce the full active and passive condition. The slope of the W-y curve between the at-rest intercept and the elastic or plastic limit is the horizontal modulus of subgrade reaction,

$$k_w = \frac{\_W/x\_}{y} \qquad . \quad . \quad . \quad . \quad . \quad . \quad . \quad . \quad . \quad . \quad . \quad . \quad . \quad . \quad (7)$$

where k_w = horizontal modulus of subgrade reaction (FL^{-3})

To date, virtually all of the research to establish values of field soil modulus have been conducted on laterally loaded vertical pile models. Attempting to extend the modulus values established in the pile research to retaining structures has been unsuccessful, and dissatisfaction is expressed in the literature regarding availability of reasonable wall values. This situation exists because of the differences inherent in soil response against a "linear" pile versus a "planar" retaining wall, such as the effect of side shear on piles, noted by Smith (30,31,33), which is clearly absent for long walls.

As previously discussed, reasonable deflection results from soil-structure interaction analysis are possible only if the quality of the soil model is compatible with the quality of the structural model. To this end, the next section of this study attempts an improvement in the value of horizontal modulus, using an analytical derivation from high-quality in-situ pressuremeter test data.

CHAPTER III

HORIZONTAL WALL MODULUS VALUES FOR COHESIONLESS SOIL
FROM PRESSUREMETER TEST RESULTS

BACKGROUND

The most difficult aspect in formulating W-y curves
for BMCOL7 input is the amount of deflection to assign to
the Wa and Wp "break points." In the elastic-plastic W-y
model, as shown in Figs. 4(c) and 4(e), for pressures
inside the plastic "envelope" a linear relationship for
horizontal pressure vs. deflection is assumed. This
relationship, the slope of the W-y curve, is commonly
referred to as the horizontal modulus of subgrade reaction.

Terzaghi's Early Work

The original development of the horizontal modulus of
subgrade reaction originates with Terzaghi's 1955 paper
(35). His notation was,

$$k_h = \frac{p}{y} \quad \cdots \cdots \cdots \cdots \cdots \cdots \cdots \cdots \cdots \cdots \quad (8)$$

where k_h = horizontal modulus of subgrade reaction

$(FL^{-3};$ Terzaghi's units are tons/cu. ft.)

p = horizontal soil pressure

y = horizontal soil displacement at p pressure

Terzaghi developed the now well-known concept that the distortion settlement of a footing is proportional to it's width, and extended this concept to laterally loaded piles and bulkhead walls. For piles, the displacement was shown to be proportional to pile width, whereas for walls the displacement is proportional to the height of the wall.

Terzaghi clearly recognized that these displacements are actually proportional to a pseudo-depth of significant stress/strain penetration, i.e. a pressure bulb, which was in turn proportional to the loaded area: footing width, pile width, and wall height. He proposed that for bulkhead walls retaining sands or gravels, k_h varied directly with a constant based only on relative density, l_h, with the depth below the free surface, z, and inversely with the total depth of wall embedment, D, as follows:

$$k_h = l_h \ \frac{z}{D} \qquad \cdots \cdots \cdots \cdots \cdots \cdots \cdots \quad (9)$$

where z = depth to point at which k_h is computed

   D = total embedded depth of wall

Terzaghi (35) also gives "empirical" values for l_h in his landmark paper. Attempting to apply Terzaghi's empirical values to real world problems is frustrating. Since l_h depends only on the relative density of the soil, k_h at the bottom of a 10-foot high and 100-foot high wall for a given soil are the same.

The Need for Better Modulus Values

It is well-known that soil stiffness in cohesionless materials increases with confining pressure and hence stiffness increases with depth. This fact is not correctly modeled by Terzaghi in Eq. 9. In the case of the BDW, using the highest I_h value given by Terzaghi for dense cohesionless soil results in a predicted wall movement of at least 18-inches before passive soil failure is reached. This much movement is about 5 times more than could intuitively be expected to result in passive wedging of the very dense granular soil in contact with this wall. Sowers (34) provides empirical coefficients that indicate the movement should about 3 to 4 inches.

Since successful application of soil-structure interaction analysis is dependent upon an accurate model of soil load-deflection response, clearly there is a need for better values than the existing empirical method. Certainly, Terzaghi never imagined that his conservative estimates of k_h would ever be applied to something as precise as the FDM analysis.

DERIVATION OF WALL MODULUS FROM THE PRESSUREMETER MODULUS

Radial Displacement in the PMT Test

The pressuremeter (PMT) test relates horizontal pressure to displacement. Baguelin et al (2) demonstrated that for plane strain around a cylindrical cavity, the

shear modulus is computed directly from the linear portion
of the pressure vs. volume change curve from the PMT test,

$$G = \frac{\Delta p}{\Delta V} V_m \quad . \quad . \quad . \quad . \quad . \quad . \quad . \quad . \quad . \quad . \quad . \quad . \quad (10)$$

where G = Shear Modulus

Δp = Change in pressure on linear portion of PMT
curve

ΔV = Change in volume over linear portion of PMT
curve

V_m = Average volume over which Δp occurs

In Eq. 10, the denominator $\Delta V/V_m$ is the
cavity volume strain over the linear portion of the curve.
Alternatively, the strain of the expanding cavity can be
measured as radial strain, as indicated in Fig. 3(a).
Radial strain can be expressed in terms of volume strain,

$$\epsilon_r = \frac{\Delta R}{R_o} = \sqrt{\Delta V/V_o + 1} - 1 \quad . \quad . \quad . \quad . \quad . \quad . \quad (11)$$

where ϵ_r = radial strain

V_o = initial PMT cavity volume

R_o = initial cavity radius

ΔR = increase in cavity radius

When the volume strain = 100% (at the arbitrarily
defined "limit pressure," the pressure required to double
the initial cavity volume), the radial strain is 41% (this

corresponds to the right-hand side of the PMT curve in Fig. 3(a), where the slope has "flattened out", and correlates with the ultimate shear strength of the soil). However, at the low volume strain associated with the linear portion of the pressuremeter curve, the radial strain is very close to 1/2 the corresponding volume strain,

$$\frac{\Delta V}{V_o} \approx 2 \frac{\Delta R}{R_o} \qquad \cdots \cdots \cdots \cdots \cdots \cdots \quad (12)$$

For these small radial strains, $V_o \approx V_m$, and substituting Eq. 12 into Eq. 10 gives the shear modulus in terms of radial strain,

$$G = \frac{1}{2} \frac{\Delta p}{\Delta R} R_o \qquad \cdots \cdots \cdots \cdots \cdots \cdots \quad (13)$$

From mechanics of materials, the modulus of elasticity is related to the shear modulus as,

$$E = 2(1 + \nu) G$$

where ν = Poisson's ratio.

The Menard (pressuremeter) Modulus, E_m, is defined as the modulus of elasticity when $\nu = 0.33$,

$$E_m = 2.66 G \qquad \cdots \cdots \cdots \cdots \cdots \cdots \quad (14)$$

where E_m = The Menard Modulus.

Substituting Eq. 14 into Eq. 13 and solving for ΔR yields the radial displacement in terms of the

Menard Modulus and the initial cavity radius,

$$\Delta R = \frac{P}{.75\ E_m}\ R_0 \quad \cdot \cdot \cdot \cdot \cdot \cdot \cdot \cdot \cdot \cdot \cdot \cdot \quad (15)$$

Further, substituting Eq. 15 into Eq. 11 yields the radial strain in terms of the Menard Modulus only,

$$\epsilon_r = \frac{\Delta R}{R_0} = \frac{P}{.75\ E_m} \quad \cdot \cdot \cdot \cdot \cdot \cdot \cdot \cdot \cdot \quad (15a)$$

Rearranging again yields the radial displacement in terms of radial strain and initial cavity radius,

$$\Delta R = \epsilon_r\ R_0 \quad \cdot \cdot \cdot \cdot \cdot \cdot \cdot \cdot \cdot \cdot \cdot \cdot \cdot \quad (15b)$$

Bearing in mind that although ΔR has been described as the increase in the cavity radius, it is also a radial displacement of the soil annulus surrounding the cavity, Eq. 15 illustrates that for a given cavity pressure, the radial displacement of the soil annulus is a function only of initial cavity radius, R_0. By similitude, for example, a cavity of 1-inch initial radius that displaces 1/4-inch radially under a given cavity pressure suggests that another cavity of 10-inch initial radius will displace 2.5-inches radially under the same pressure increase in the same soil.

Flat Plate vs. Radial Displacement

The deformation of the soil behind a retaining wall can be idealized as the strain of the soil in contact with the face of the wall, multiplied by some gage distance,

$$y = \epsilon_w R_w \qquad \ldots \ldots \ldots \ldots \ldots \ldots \ldots \quad (16)$$

where ϵ_w = strain of soil in contact with the wall.

R_w = equivalent gage distance into soil mass

behind wall over which ϵ_w produces y.

Note the similarity between Eq. 15b and 16. In each equation, a displacement is equal to a strain times a gage length. Eq. 16 can be visualized as a "flat-plate" version of Eq. 15b, wherein the pressuremeter cavity has been conceptually sliced longitudinally and "unwrapped" to a flat wall shape.

The next step in relating displacement behind a wall, y, to radial displacment in the PMT test, ΔR, is to find the relationship between the strains, ϵ_r and ϵ_w.

A soil element in the annulus around an expanding PMT cavity displaces in the tangential, or Θ, as well as the radial, or r, direction. Following Baguelin's (2) procedure of simplifying the problem to an elastic-plastic model, radial and tangential strains are assumed to be approximately equal over the range of small displacements associated with the linear portion of the PMT curve, as

shown in Fig. 5(a), i.e.,

$$\epsilon_r \approx \epsilon_\Theta$$

However, behind a long retaining wall, soil elements cannot expand in a direction parallel to the wall, due to continuity with neighboring elements. Therefore, ϵ_w in Eq. 16 must be adjusted by ν to relate it to ϵ_r from the PMT test. From the definition of Poisson's ratio, and as shown in Fig. 5(b),

$$\epsilon_w = \epsilon_r - \nu \epsilon_r$$
$$= \epsilon_r (1-\nu) \qquad \ldots \ldots \ldots \ldots \ldots \ldots (17)$$

Substituting Eq. 15a into Eq. 17,

$$\epsilon_w = \frac{p}{.75 \ E_m} (1-\nu) \qquad \ldots \ldots \ldots \ldots \ldots (18)$$

Substituting Eq. 18 into Eq. 16 gives wall displacement, y in terms of the pressuremeter modulus and wall gage length,

$$y = \frac{p}{.75 \ E_m} (1-\nu) \ R_w \qquad \ldots \ldots \ldots \ldots (19)$$

Scaling-Up the PMT Probe to a Real Wall

Intuitively, if Rw in Eq. 19 is replaced by Ro, the result is a relationship between pressure p and displacement y for a flat plate the size of the unwrapped PMT probe.

Consistent with Terzaghi's general idea that the displacement of a bulkhead wall is proportional to it's
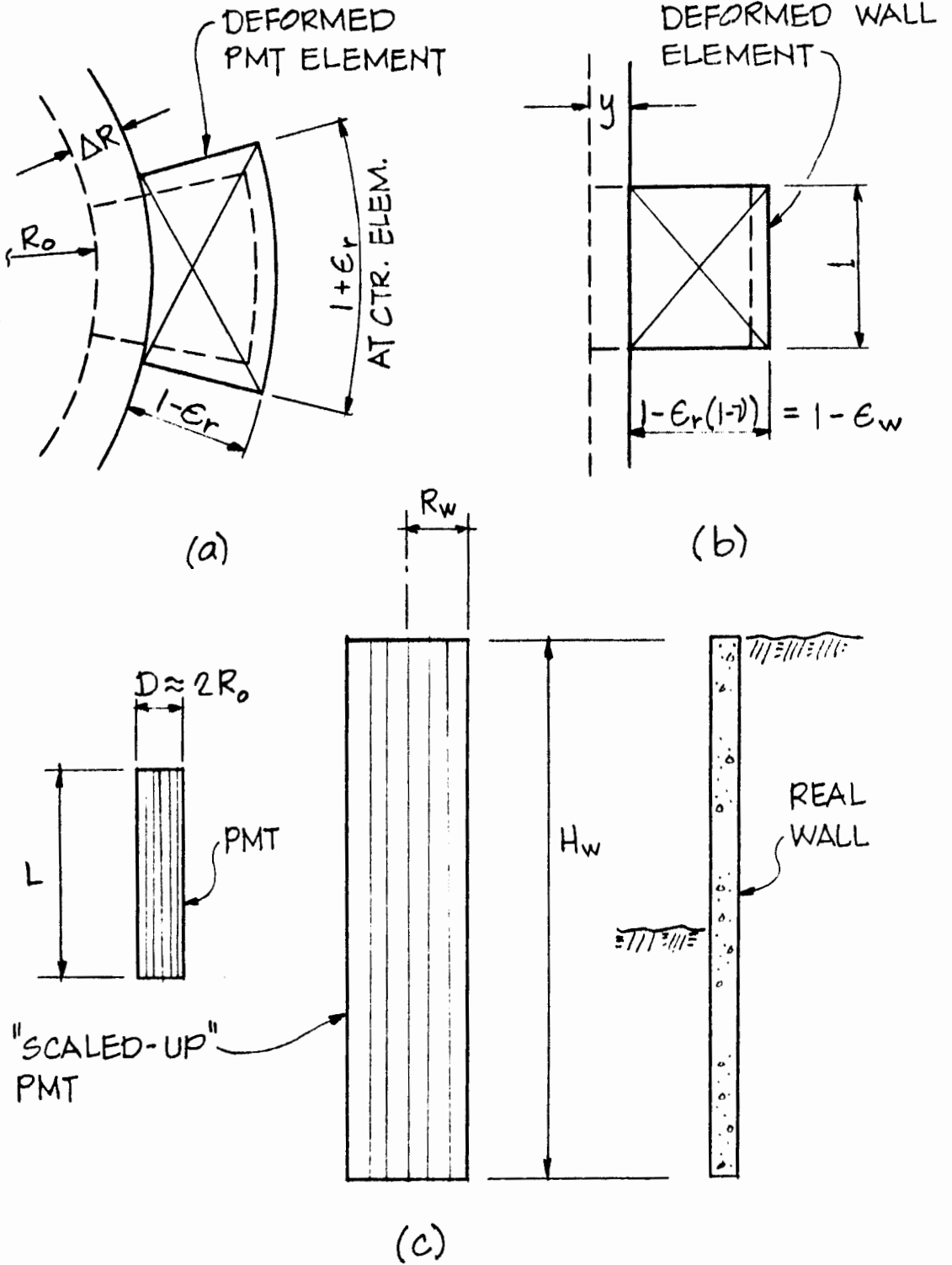
Figure 5. Deformation of a unit soil element behind the face of (a) a PMT cavity, (b) a wall, and (c) scaling-up the PMT probe to a real wall.

embedment or heighth, Eq. 19 can be applied to a real wall if the unwrapped PMT is conceptually "scaled-up" so the probe length is equal to the height of the wall, maintaining the same L/D ratio of the probe actually used. Clearly, R_W in Eq. 19 becomes the "scaled-up" R_O. As shown in Fig. 5(c),

$$\frac{L}{D} = \frac{H_W}{2 R_W} \quad \cdots \cdots \cdots \cdots \cdots \cdots \quad (20)$$

where L = pressuremeter probe length

D = initial pressuremeter diameter = $2R_O$

Hw = height of the retaining wall

Briaud et al (4) demonstrated that any probe with an L/D ratio of 5 or more produces a response very close to the plane strain assumed in all current pressuremeter theory. Since a shorter probe will not produce the assumed plane strain conditions and should therefore not be used, and since a longer probe will produce the same plane strain conditions achieved in an L/D = 5 probe, L/D = 5 should be used in Eq. 20, rather than the L/D of the actual probe used. Making this substitution in Eq. 20,

$$R_W = \frac{H_W}{10} \quad \cdots \cdots \cdots \cdots \cdots \cdots \cdots \quad (21)$$

Substituting Eq. 21 into Eq. 19 gives an expression for wall displacement in terms of applied pressure, pressuremeter modulus, and height of wall,

$$y = \frac{p}{.75 \; E_m} \; (1-\nu) \; \frac{H_w}{10} \qquad \cdots \cdots \cdots \cdots \quad (22)$$

The PMT Wall Modulus

Substituting Eq. 22 into Eq. 8, and changing the modulus notation from k_h to k_w, to indicate the application to walls, gives a final expresssion for wall modulus in terms of pressuremeter modulus, poissons ratio, and height of wall,

$$k_w = \frac{7.5}{(1-\nu)} \; \frac{E_m}{H_w} \qquad \cdots \cdots \cdots \cdots \cdots \quad (23)$$

Eq. 23 represents the horizontal modulus of subgrade reaction corresponding to E_m at a specific elevation on a wall of height H_w. It can be seen from Fig. 6, for the usual values of ν for soils, that $k_w(H_w)/E_m$ varies from about 10 to 15. For soils in which ν is approximately .33, a value from 10 to 12 should be used. For the BDW, a value of 10 was used, in conjunction with Eq. 7, to establish the W-y curves used in Chapter IV, as follows,

$$k_w = 10 \; \frac{E_m}{H_w} \qquad \cdots \cdots \cdots \cdots \cdots \cdots \quad (24)$$
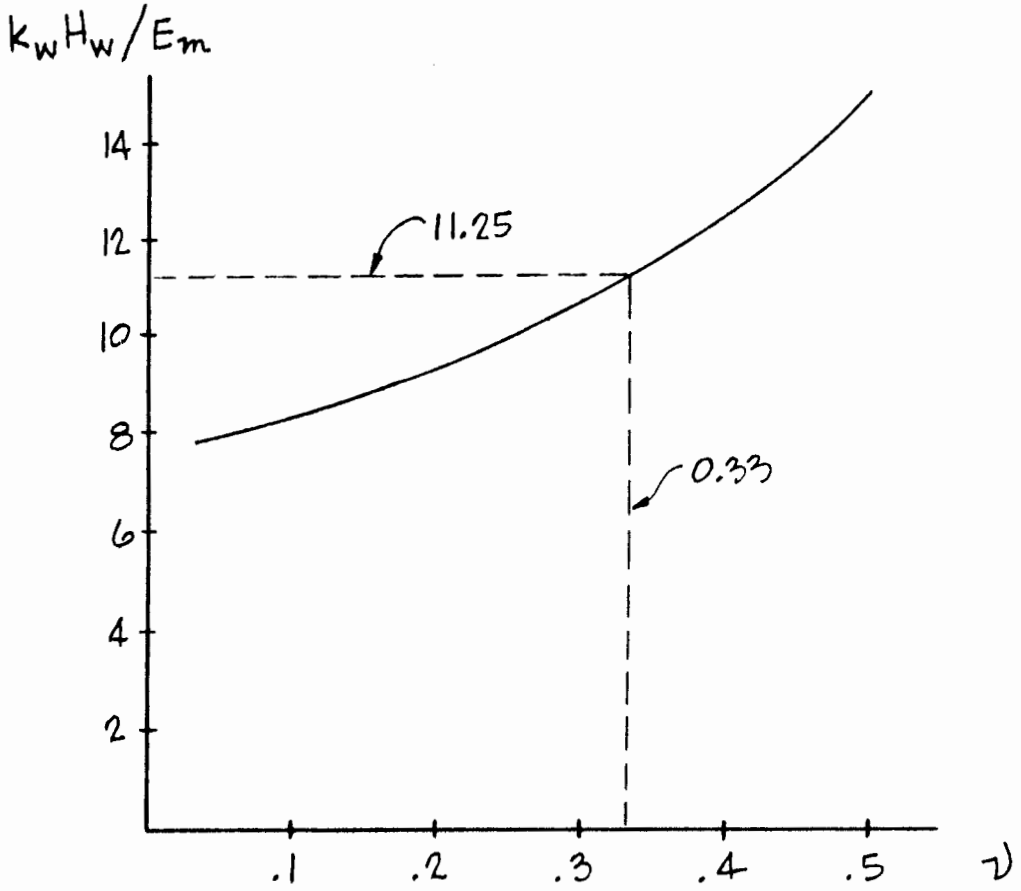
Figure 6. $(k_w H_w)/E_m$ vs. Poisson's Ratio, ν.

Comparing the PMT Wall Modulus to Terzaghi

Since the pressuremeter modulus E_m normally increases linearly with depth for sands and gravels, Eq. 23 was re-written to appear similar to Terzaghi's notation from Eq. 9, making a change from I_h to I_w, once again to indicate that the application is for walls,

$$k_w = \frac{7.5}{(1-\nu)} \frac{E_m}{z} \frac{z}{H_w}$$

$$= I_w \frac{z}{H_w} \quad \quad \cdots \quad \cdots \quad \cdots \quad (25)$$

where $I_w = \frac{7.5}{(1-\nu)} \frac{E_m}{z}$

$\frac{E_m}{z}$ = variation of Menard Modulus with depth.

In order to compare Terzaghi's k_h with k_w, a hypothetical 15-foot high wall retaining cohesionless sand was considered. The amount of movement required to reach full passive resistance at the base of the wall, y_p, was computed both methods and compared with empirical coefficients from Sowers (34). The results of this comparison are tabulated in Table I.

From the empirical wall movement coefficients given by Sowers (34), the expected movement to mobilize passive resistance is between .005 and .01 of the wall height, or .90 to 1.80-inches. It is apparent that k_w yields a displacement within these bounds, whereas the values of movement from Terzaghi's k_h are 4 to 5 times too high.

Similarly, it was previously noted that movements on the order of at least 18-inches are required, using Terzaghi's k_h, to reach full passive resistance in the BDW. This movement becomes more reasonable, about 3-inches, when k_w is used, as shown in Chapter IV.

TABLE I

EXAMPLE 15-FOOT HIGH WALL RETAINING COHESIONLESS SAND

Rel. Density:	LOOSE	MEDIUM	DENSE
ϕ', degrees:	25	30	35
K_p	4	6	8
γ, pcf	90	110	120
TERZAGHI:			
l_h, tcf	4	8	20
k_h, pci	5	9	23
y_p, inches	7.5"	7.6"	4.4"
k_w from PMT:			
E_m, kPa	3000	8000	15,000
k_w, pci	23	62	116
y_p, inches	1.6"	1.1"	0.9"
SOWERS:			
y_p	1.8"	1.4"	0.9"

CHAPTER IV

A PARAMETRIC STUDY OF A SECTION OF THE
PERMANENT BUTTRESS DIAPHRAGM WALL

THE BUTTRESS DIAPHRAGM WALL, STATION 17+00 TO 19+60

The section of the BDW selected for the parametric
soil-structure interaction study lies between stations
17+00 and 19+60, at the west end of the BDW, near the SE
corner of the actual lock structure.

Geometry and Design

This section of wall, BDW 17+00 to 19+60, is
potentially critical for deflections. It has the greatest
elevation from top of wall to dredge line, 51-feet. In
addition, this part of the wall is within the lock
construction coffer-dam, and will be excavated in the dry,
resulting in higher outward pressures against the wall than
will be generated for the other stations, which will be wet
dredged.

The geometry and cross sectional properties of BDW
17+00 to 19+60, as the design stood in January, 1987, were
provided by the USACE in January, 1987. The geometry is
summarized in Fig. 7. A summary of wall cross-section
structural properties is given in Table II.
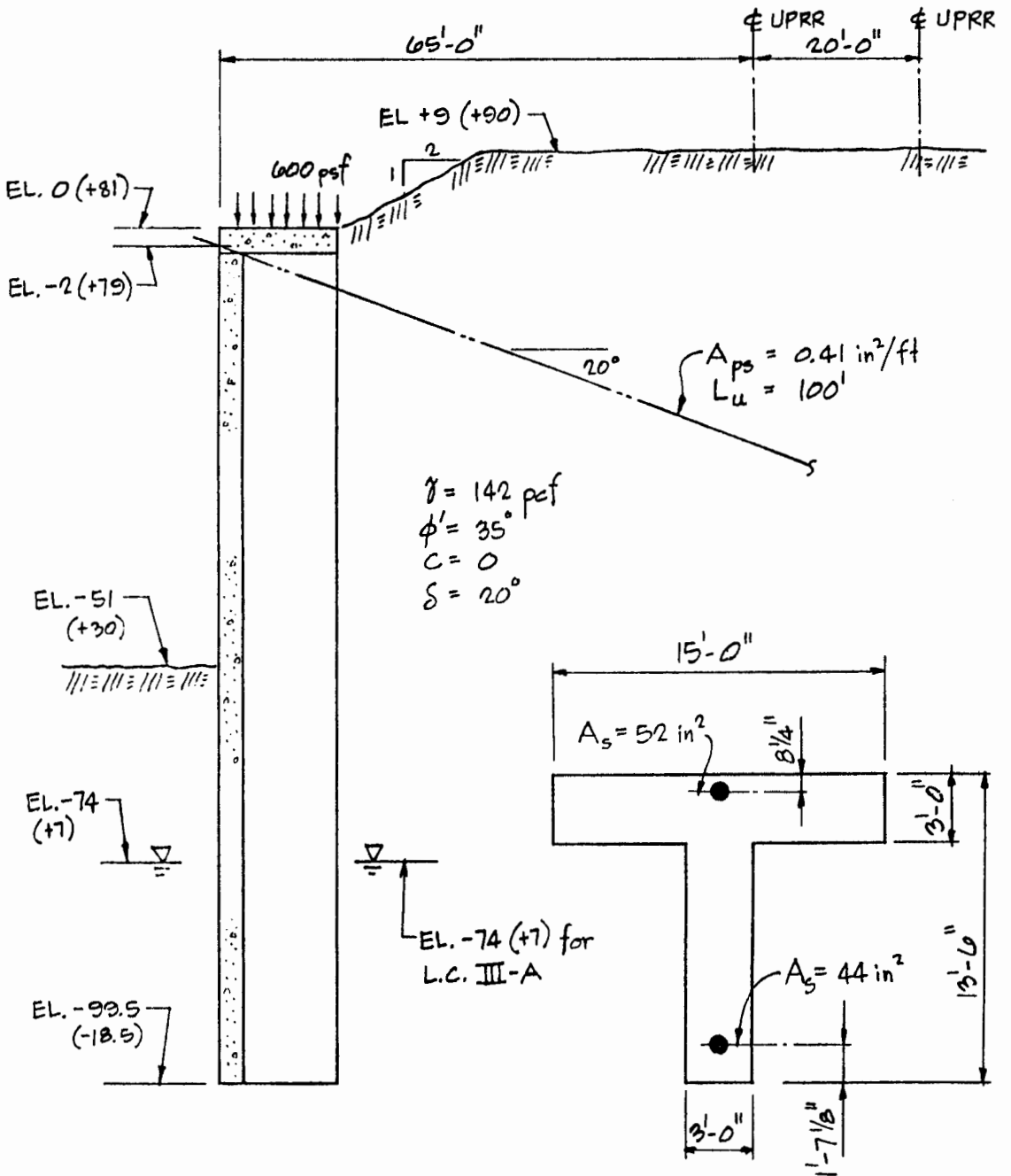
Figure 7. Bonneville BDW, Sta. 17+00 to 19+60.

Throughout this study, elevations are referred to El. 0 at the top of the wall. In Fig. 7, a second set of elevations are given in parentheses, which correspond to the reference elevations used by the Corps.

TABLE II

STRUCTURAL PROPERTIES OF BDW STA. 17+00 TO 19+60

STRUCTURAL PROPERTY	VALUE
Concrete strength, $f'c$	6000 psi
Gross section stiffness, EI_g	7.1×10^{12} #-in^2/ft
Cracked section stiffness, EI_{cr}	1.7×10^{12} #-in^2/ft
Stem cracking moment, M_{cr} (-)	706 k-ft/ft
Flange cracking moment, M_{cr} (+)	1,521 k-ft/ft
Area of tie-back anchors, A_{ps}	0.41 in^2/ft
Effective length of anchors, L	100 ft
Strength of tieback anchors, f_{pu}	270 ksi
Anchor prestress level, f_{ps}	$0.45 \times f_{pu}$
Anchor preload, horiz. component	49.8 k/ft

Loading Condition III-A

For the parametric study, one critical loading condition was used: L.C. III-A, a dewatered construction loading condition. Additionally, we have imposed final

embankment surcharge loads while the wall remains in the
dewatered condition. The sequence of construction and
loading events modeled are as follows:

1. The railroad embankment shown on Fig. 7 is in place.

2. The wall is constructed in-place by slurry techniques.

3. The coffer dam is constructed, and both sides of the
   wall are dewatered to El. -74, and will remain
   dewatered throughout this sequence.

4. The channel-side of the wall is excavated to El. -5,
   the tieback anchors are installed at El. -2, and the
   anchors are preloaded.

5. The channel-side of the wall is excavated in the dry
   to El. -51.

6. The railroad embankment is subjected to the two 16,000
   lb/ft railroad line loads.

7. The surface of the retained soil behind the wall is
   subjected to a 600 psf equipment surcharge.

SOIL PROPERTIES AT THE BDW FROM PMT RESULTS

The soil model used in this study was derived in part
from the "Pressuremeter Testing and Design Interim Report",
Smith (30), which includes a discussion of material
behavior, strength characteristics, and design
considerations, as well as a comprehensive set of
high-quality pressuremeter test results.

Mohr-Coulomb Parameters

The materials retained by the BDW can be considered, from a conservative design standpoint, as a coarse, angular gravel. The material is assumed cohesionless, with all design based on drained behavior. Initial horizontal (K_o) ground stresses are probably in excess of overburden pressure, due to the high stresses mobilized from inertia forces to reach equilibrium in the ancient slide. A summary of the "Mohr-Coulomb" strength parameters taken from the report for use in this study are given in Table III.

TABLE III

GEOTECHNICAL PROPERTIES FOR SB MATERIAL AT THE BDW FROM THE PRESSUREMETER TESTING AND DESIGN INTERIM REPORT

GEOTECHNICAL PROPERTY	VALUE
Effective friction angle, ϕ'	35 degrees
Cohesion, c'	0
Unit weight, γ	142 pcf
Submerged unit weight, γ'	80 pcf
At-rest coefficient, K_o	1.0 to 1.5

after Smith (30)

The Pressuremeter Modulus

Pressuremeter tests conducted in SB (slide block) materials in drill hole DH 1751 show the expected linear increase of pressuremeter modulus with increase in depth. This data is plotted, and a straight line fit made to establish Em vs. depth, in Fig. 8. From this fit, a value for the rate of increase in Em of 320 psi per foot of depth was found.

ANALYSIS PROCEDURE

W-Y Curves

Parameters were derived from Table III and Fig. 8 for direct use in computing the W-Y curves for the wall. Active and passive pressure coefficients were derived from Eqs. 5 and 6, using a wall friction value from (24). The wall modulus, k_w, was determined from Fig. 8 and Eq. 24. A summary of the derived values is shown in Table IV.

The 2-Stage Procedure

The soil-structure interaction analysis was conducted by making 2 separate runs on BMCOL7. This procedure, the first documented attempt to accurately model deflections in staged slurry-wall construction, was devised because the tieback anchors are preloaded prior to excavation of the channel side of the wall. The soil pressure vs. wall deformation response during preload is different from, and
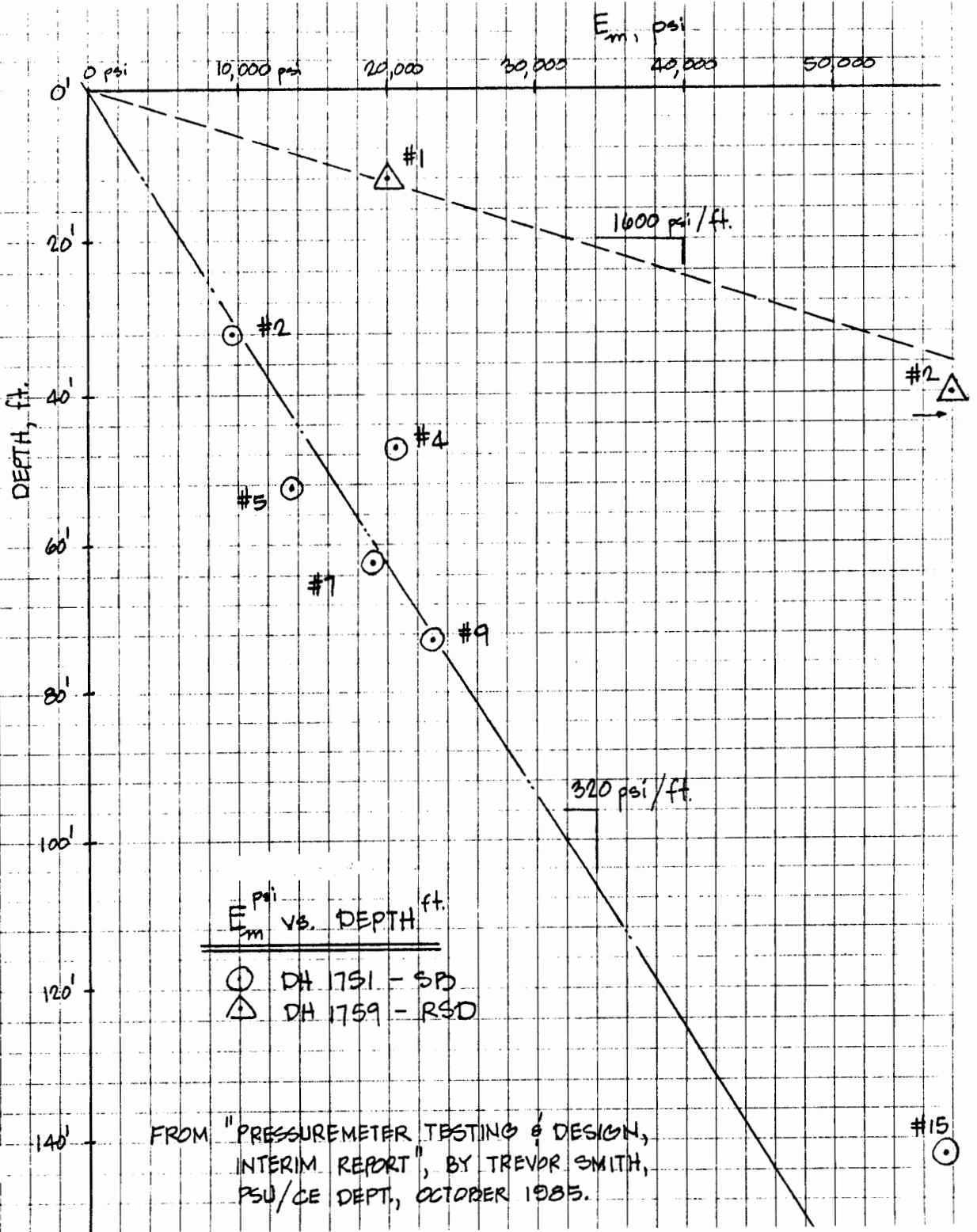
Figure 8. Pressuremeter modulus vs. depth.

influences the result of, the response after excavation. Another way of visualizing this effect is that not only is the anchor prestressed, but also the soil is precompressed during preloading.

TABLE IV

PARAMETERS DERIVED FROM THE PMT RESULTS USED TO DEVELOP THE W-Y CURVES FOR THE BDW.

PARAMETER	VALUE
Wall friction angle, ∂	20 degrees
Active pressure coefficient, K_a	0.25
Passive coefficient, K_p	8.0
PMT modulus increase, E_m	320 psi/ft
Wall horizontal modulus, k_w	4600 pcf/ft

This procedure requires hand generation of two complete sets of W-Y curves, the set for the second run based on the outcome of the first. An example of this procedure is illustrated in Fig. 9, which shows a schematic representation of BDW 17+00 - 19+60 at the first and second stage of analysis, with corresponding W-Y curves at El -20.

The first stage, shown on the top half of Fig. 9, corresponds to anchor preloading, as described in Step 4 under Loading Condition Analyzed, above. Channel side

W-Y CURVE EXAMPLE

$F_{P/L} = 49.8^K$, $K_o = 1.0$, $k_w = 4600z$, $A_{ps} = .41$

PRELOAD W-Y CURVE @ -20'

49.8^K PRELOAD

$-2.98''$

$W_p - W_a = +16,300$ psf

$W_o - W_o = -829$ psf

$\frac{W_p - W_a - W_o}{k_h} = +2.91''$

$W_p - W_a = -23,140$ psf

BMCOL7 PRELOAD
SOLUTION @ -20' ⟹ W = -1827 psf; y = +0.13''

FINAL EXCAV. W-Y CURVE @ -20'

16^K 16^K

600 psf

$A_{ps} = 0.41$ in², L = 100'

$-.31''$
$W_a = -783$ psf

$W_o = -3151$ psf

-1827 psf

FROM P/L SOL'N.

0.17''

$+2.88''$

$W_p = -25,208$ psf

BMCOL7 FINAL EXCAV. SOLUTION ⟹ W = -1549 psf; y = -.0377

FINAL $\Delta_{20'} = +.13'' - .0377'' = +.092''$
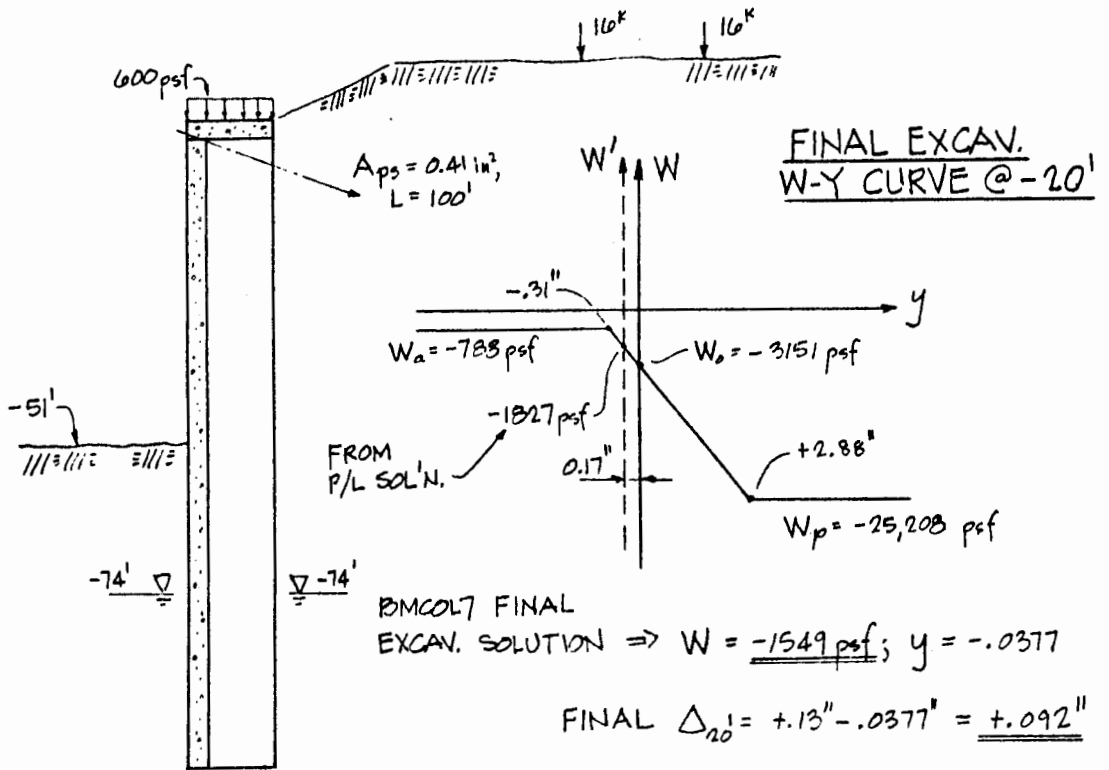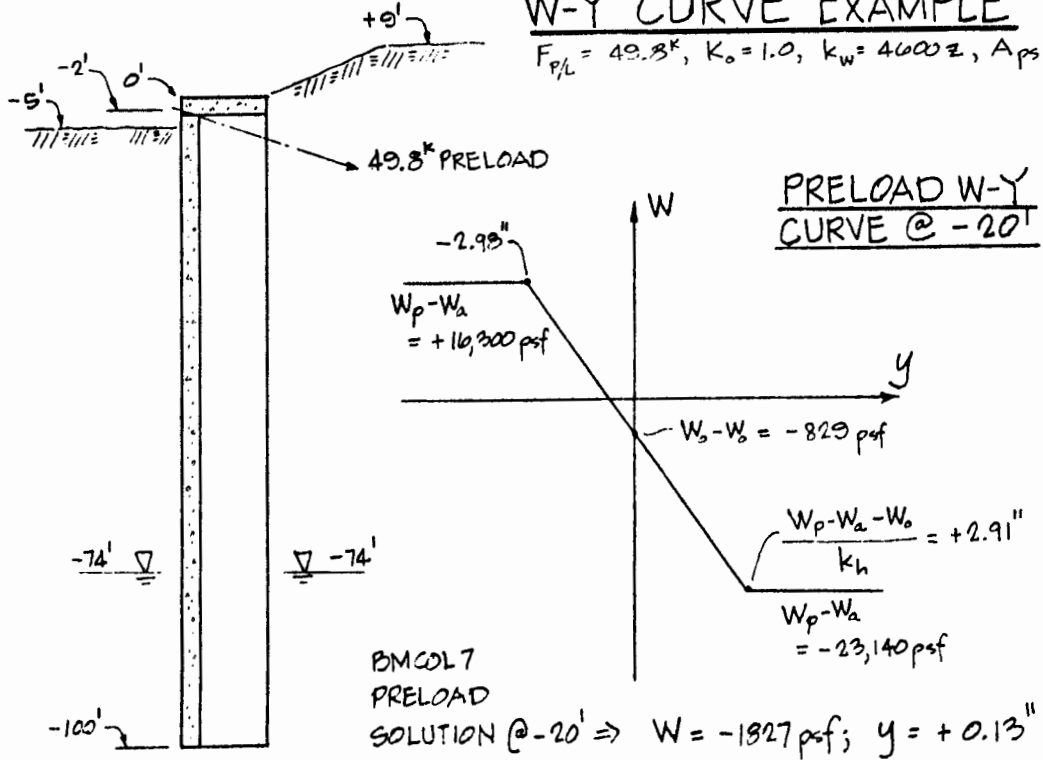
Figure 9. W-y curve example.

excavation is assumed to El -5, to allow for installation
of the anchors; the railroad embankment has been
constructed to El. +9. The W-Y curve shows that before any
movement occurs (i.e., Y = 0), there is a net (resultant)
pressure on the wall of -829 psf, corresponding to the
difference in at-rest pressures on each side of the wall at
El. -20; note that the (-) indicates the resultant pressure
is directed toward the channel side, because the small
excavation on that side has reduced vertical overburden and
hence in-situ horizontal pressures on the channel side.
Movements in excess of 2.98-inches toward the channel side
mobilze full passive resistance of the soil on that side of
the wall (less active pressure from the hill side).
Movements in excess of 2.91-inches toward the hill side are
resisted by the passive pressure from the hill side soil,
less the active pressure from the channel side. The
2.91-inches of movement to reach full passive resistance
was computed by subtracting the net at-rest pressure on the
wall from the passive-active resultant, and dividing by the
wall modulus, k_w, which was determined by multiplying
the value in Table III by 20-feet. W-Y curves were
established in likewise fashion at approximately every
10-feet of wall elevation, for input into the BMCOL7
analysis, along with the anchor preload. The result of this
analysis indicates a resultant pressure at El -20 of -1827
psf, corresponding to a deflection of +0.13-inches. These

numbers can be checked for consistency on the W-Y curve.

The second-stage of analysis is shown on the bottom half of Fig. 9, corresponding to full excavation to El. -51 on the channel side, and the addition of railroad line load and distributed equipment surcharge loads, as described in the final Step 7 under Loading Condition Analyzed, above. A completely different W-Y curve must now be established at El. -20, because the soil resistance on the channel side is gone. This new curve is computed in similar fashion as previously described, but using the active, at-rest, and passive values of the hill side soil mass only. One additional step is required: the result of the first stage must be incorporated, since preloading the anchor also in effect preloads the soil. This effect is incorporated by moving the W-axis of the stage-2 W-Y curve so the Y=0 pressure corresponds to the pressure the soil sees at the end of preload --- in this case, -1827 psf.

Final deflections are established by superimposing the values from stage-1 and stage-2; this is necessary because stage-2 was run with what amounts to preloaded pressures from stage-1, but starting with a new datum for deflections. This superposition is not required for final pressures, shears and moments, since the preloaded soil pressure has been incorporated by the shift of the W-axis previously described.

THE PARAMETRIC STUDY

Five parameters were studied for their effect on deflection, bending moment, and passive soil failure. They were anchor preload, anchor stiffness, wall section stiffness, soil at-rest pressure coefficient, and horizontal modulus.

In order to determine the influence in the variation of each parameter, they were varied one at a time from a control configuration, consisting of a "Best Estimate" (BE) of each parameter, as tabulated in Table V.

The variation of the selected parameters is shown in Table VI. In effect, Table V represents a single configuration analyzed, and Table VI represents 7 additional analyses, with a parameter varied one at a time.

TABLE V

BEST ESTIMATE VALUE OF PARAMETRIC STUDY VARIABLES.

PARAMETER	BEST ESTIMATE VALUE
Anchor preload, horiz. component	49.8 k/ft
Section stiffness, $EI = EI_g$	7.1×10^{12} #-in^2/ft
Area of tie-back anchors, A_{ps}	0.41 in^2/ft
At-rest pressure coefficient, K_o	1.0
Wall horizontal modulus, k_w	4600 pcf/ft

TABLE VI

VARIATION OF "BEST ESTIMATE" PARAMETERS.

PARAMETER	VALUE VARIED from "BEST ESTIMATE"
Anchor preload, horiz. component	24.9 k/ft, 0
Section stiffness, $EI = EI_{cr}$	1.7×10^{12} #-in^2/ft
Area of tie-back anchors, A_{ps}	0.205 in^2/ft
At-rest pressure coefficeint, K_o	0.5, 1.5
Wall horizontal modulus, k_w	2300 pcf/ft

Anchor Preload

The Best Estimate value of the tieback anchor preload corresponds to the intended preload of 0.45 x f_{pu} x A_{ps} = 49.8 kips/ft. Two other analyses were made, one with one-half that value, 24.9 kips/ft, and one with no preload. The results of these runs are shown graphically in Figs. 10, 11, and 12. The left diagram in these Figures shows resultant soil pressure vs. height of wall, and the right hand diagram shows deflection and bending moment vs. height of wall. For the pressure and deflection values, two curves are shown: one is at the end of preload (stage-1), with the second after excavation and application of surcharge loads (stage-2).

$A_{ps} = .41 \ ^{in^2}/ft$
$F_i = 49.8^k$
$F_f = 48.99^k$

EXCAVATION AT PRELOAD, $-5'$

1827 psf

PRESSURE AFTER P/S

FINAL PRESSURE

FINAL DREDGE LINE $-51'$

1920 psf

965 psf

SCALE:
500 psf

PRELOAD = $.45 f_{pu}$
$K_o = 1.0$
$k_w = 4600 \ z \ pcf$
$A_{ps} = 0.41 \ in^2/ft.$

.316" .412"

DEFLECTION AFTER P/S, BEFORE EXCAV.
$+895^{k'}$

FINAL MOMENT

$-.151"$

FINAL DEFLECTION

$-.0515"$

SCALE:
0.10"   100 K-FT.

Figure 10. Preload = .45 × f_{pu}.

EXCAVATION
AT PRELOAD,
-5'

$A_{ps} = .41 \text{ in}^2/\text{ft}.$
$F_i = 24.9^k$
$F_f = 28.5^k$

-.283"

+.081"

DEFLECTION
AFTER P/S,
BEFORE EXCAV.

925 psf

FINAL
DEFLECTION

-.364"

+659 k'

FINAL
EXCAVATION,
-51'

1920 psf

FINAL
PRESSURE

1236 psf

-.53"

FINAL
MOMENT

PRESSURE
AFTER P/S,
BEFORE EXCAV.

SCALE:

500 psf

SCALE:

0.10"   100 k'

$\underline{PRELOAD = .225 \, f_{pu}}$

$K_o = 1.0, \quad A_{ps} = 0.41 \text{ in}^2/\text{ft}$

$k_w = 4600 \, z$

Figure 11. Preload = .225 × f_{pu}.

Figure 11. Preload = $.225 \times f_{pu}$.

$A_{ps} = .41^{in^2/ft}$
$F_i = 0$
$F_f = 31.96^k$

−3.28"

FINAL
DEFLECTION

−2.6"

FINAL DREDGE
LINE, −51'

1920 psf

−1.88"

1650 psf

FINAL
PRESSURE

787$^{k'}$

FINAL
MOMENT

2465 psf

SCALE:

500 psf

PRELOAD = 0
$K_J = 1.0$, $A_{ps} = .41^{in^2/ft.}$
$k_w = 4600 z$

SCALE:

1.0"   100^{k-ft}

3000 psf

Figure 12.   Preload = 0.

Final (stage-2) deflection curves for the 3 preload
conditions are superimposed on one diagram for comparison
in Fig. 13 (note that the curve showing + 0.41-inches at
the top of the wall corresponds to the "Best Estimate"
configuration; this curve will re-appear for reference on
subsequent diagrams in this report). Final moment curves
for the 3 preload conditions are superimposed on Fig. 14.

Section and Anchor Stiffness

Although none of the first 3 runs investigating
anchor preload variations resulted in a maximum bending
moment that was in excess of wall section cracking moment,
an additional run was made of the Best Estimate
configuration with a fully cracked wall stiffness, for the
full height of the wall. This was done for correlation
with USACE analyses, which were made assuming a cracked
section, which could exist along the wall from causes other
than bending stress.

Another "structural" variation of interest is the
effect of tieback anchor slip on deflection. A more
flexible anchor can be modeled by changing the
cross-section area of the anchor. To model a slipping, and
hence flexible anchor, a run was made of the "BE"
configuration, but with one-half the anchor load, i.e. 24.9
Kips/ft, and one-half the anchor area, i.e. 0.205 in2/ft.

Deflections resulting from these reductions in wall

-3.3"

-.28"
FINAL Δ,
PRELOAD
= 0.225 f_{pu}

+.41"
FINAL Δ,
PRELOAD
= 0.45 f_{pu}

EXCAV @ PREL'D.
-5'-0

0'

10'

FINAL Δ,
PRELOAD = 0

-2.6"
@ -25'

20'

-.36"
@ -30'

30'

40'

FINAL
EXCAVATION, -51'

-1.9"
@ -50'

50'

-.15" @ -55'

60'

PRE-PRELOAD and
PRE-EXCAVATION
DATUM LINE

70'

K_o = 1.0
k_w = 4600 ± pcf
A_{ps} = 0.41 in²/ft.

80'

BDW STA. 17+00 - 19+60

90'

DEFLECTION vs. PRELOAD

L.C. III-A   GWL = -74' EA. SIDE

SCALE: 5' ⊢——⊣ ½"

-.25"

100'
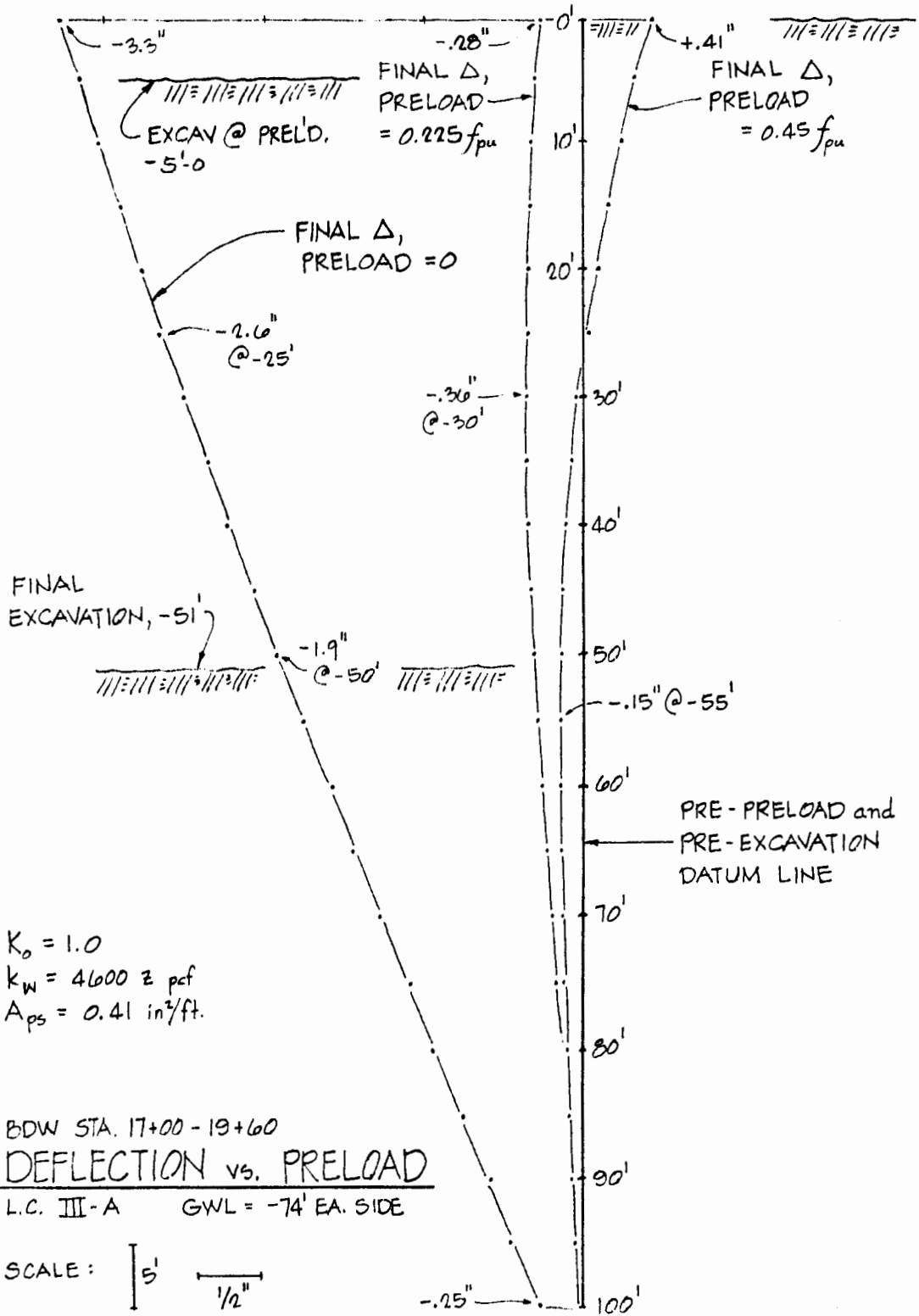
Figure 13.   Deflection vs. Preload.

EXCAV. @ PRELOAD
−5'

MOMENT DIAGRAMS
SHOWN ARE "FINAL" −
AFTER PRELOAD and
EXCAVATION.

FINAL
EXCAVATION, −51'

PRE − PRELOAD and
PRE − EXCAVATION
"O − MOMENT" LINE

$660^{k'}$ @ −38'
(PREL'D = $.225 f_{pu}$)

$895^{k'}$ @ −40'
(PRELOAD = $.45 f_{pu}$)

$790^{k'}$ @ −40'
(PRELOAD = 0)

M_{cr} = 1,521 $^{k'}$

K_o = 1.0
k_w = 4600 z pcf
A_{ps} = 0.41 in²/ft.

BDW STA. 17+00 − 19+60

MOMENT vs. PRELOAD

L.C. III − A   GWL = −74' EA. SIDE
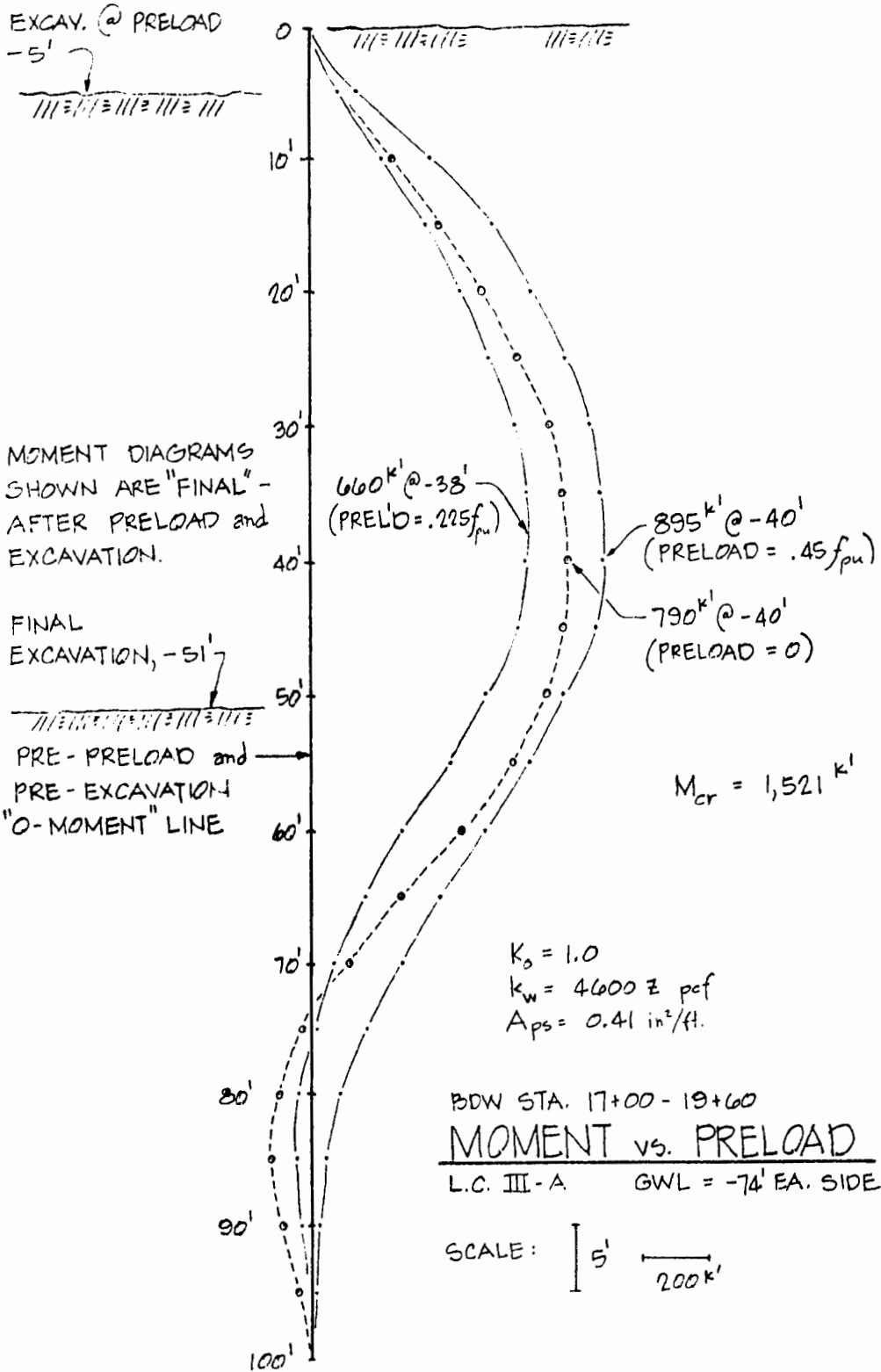
SCALE: 5'   200$^{k'}$

Figure 14.   Moment vs. Preload.

section and tieback anchor stiffness are shown graphically
on Fig. 15, along with the Best Estimate deflection curve
for reference.

In-Situ At-Rest Pressure

The in-situ at rest, or K_O, pressure is probably
the most difficult parameter to reliably estimate, since
it's value is hard to measure, and dependent upon geologic
depositional conditions. Hence, investigation of
variations in K_O are of importance, owing to it's
uncertain nature.

K_O could vary from as low as 0.4, a value
corresponding to sand loosely deposited in horizontal
layers without compaction, to about 1.5, as suggested by
Smith (30). BMCOL7 runs were made with K_O of 0.5, 1.0,
and 1.5. The resulting final (stage-2) deflection for these
3 configurations are plotted in Fig. 16. Note that the
curve for K_O = 1.0 is also the reference Best Estimate
value.

Horizontal Wall Modulus

The horizontal wall modulus, k_W, was derived from
pressuremeter results from DH 1751, using the method
derived in the third section of this thesis. For this
study, a value of 4600 pcf/ft was found. To study the
influence of this value on deflection, a BMCOL7 run was
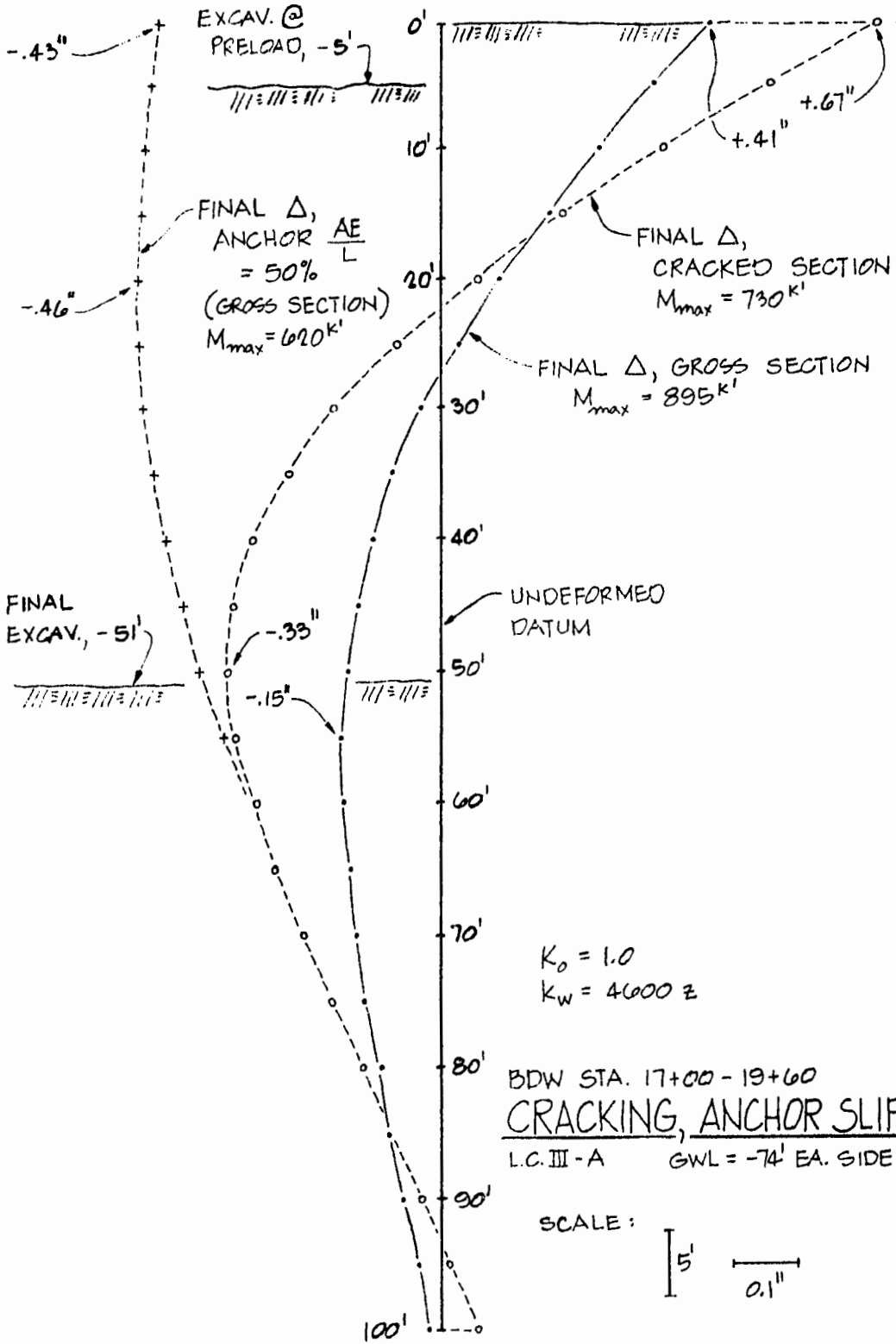made with One-half of the derived stiffness value. The

Figure 15. Cracking, anchor slip.
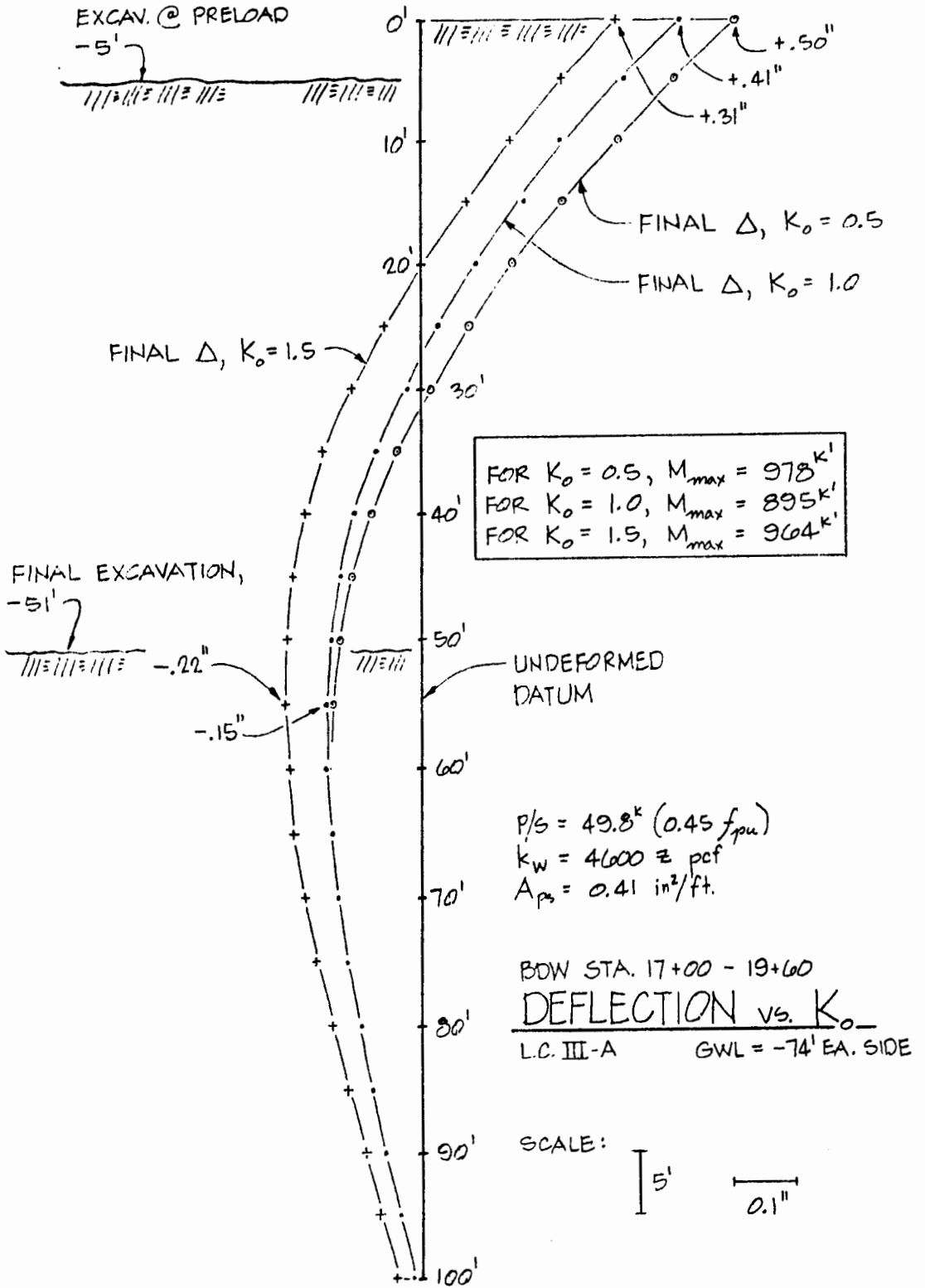
Figure 16. Deflection vs. K_o.

resulting final (stage-2) deflection is plotted, along with the Best Estimate deflection curve, in Fig. 17.

SUMMARY OF RESULTS

A tabular summary of results of the Best Estimate configuration, showing final (stage-2) anchor force, maximum moment, and deflections at the top of the wall and near the dredge line, are shown in Table VII. A similar tabulation of the 7 "one-at-a-time" parametric variations follows in Table VIII.

Effect of Parameters on Deflection

A graphical display of the effect of preload, K_O, and k_W on the deflection at the top of the wall, and at the dredge line, is shown in Fig. 18.

Effect of Parameters on Moment and Anchor Force

A graphical display of the effect of preload, K_O, and k_W on top of wall and dredge line deflection is shown in Fig. 19.

Effect of Parameters on Passive Factor of Safety

A graphical display of the effect of preload, K_O, and k_W on soil passive failure factor of safety is shown in Fig. 20.

EXCAV. @ PRELOAD −5'

FINAL Δ, $k_w = 4600 \mp$ pcf

FINAL Δ, $k_w = 2300 \mp$ pcf

+.55"

+.41"

FOR $k_w = 4600$, $M_{max} = 895^{k'}$
FOR $k_w = 2300$, $M_{max} = 1,055^{k'}$

FINAL EXCAVATION −51'

−.15"

UNDEFORMED DATUM

−.23"

$P/S = 49.8^k$
$K_o = 1.0$
$A_{ps} = 0.41$ in²/ft.

BDW STA. 17+00 − 19+60
DEFLECTION vs. k_w
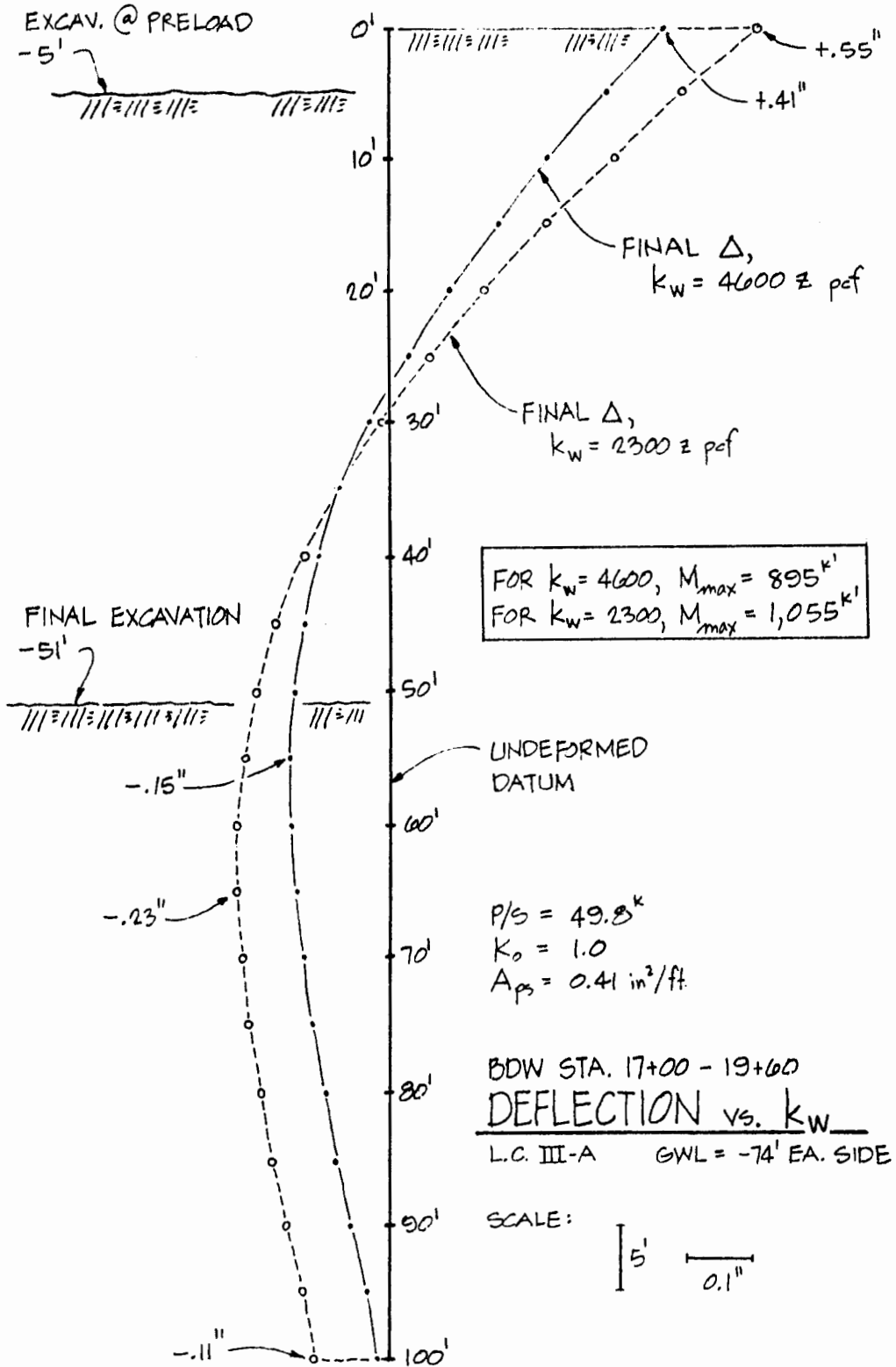L.C. III-A   GWL = −74' EA. SIDE

SCALE:

5'   0.1"

−.11"

Figure 17.   Deflection vs. k_w.

TABLE VII

FINAL (STAGE-2) ANCHOR FORCE, MAXIMUM MOMENT, AND DEFLECTION
FOR THE BEST ESTIMATE PARAMETRIC CONFIGURATION

preload = 49.8, A_{ps} = .41, EI = EI_g, K_o = 1.0, k_w = 4600z

	ANCHOR FORCE	MAXIMUM MOMENT	Δ TOP OF WALL	Δ DREDGE LINE
BEST ESTIMATE	49.0 k	895 k'	+ .41"	- .15"

TABLE VIII

FINAL (STAGE-2) ANCHOR FORCE, MAXIMUM MOMENT, AND DEFLECTION
FOR PARAMETRIC VARIATIONS FROM BEST ESTIMATE

	ANCHOR FORCE	MAXIMUM MOMENT	Δ TOP OF WALL	Δ DREDGE LINE
PRELOAD = 24.9	28.5	659	- .28	- .36
PRELOAD = 0	32.0	787	- 3.28	- 1.9
PRELOAD = 24.9; A_{ps} = .205	27.4	620	- .43	- .37
EI = EI_{cr}	46.7	730	+ .67	- .33
K_o = 0.5	48.8	978	+ .50	- .15
K_o = 1.5	49.2	964	+ .31	- .22
k_w = 2300 z	49.0	1,055	+ .55	- .23
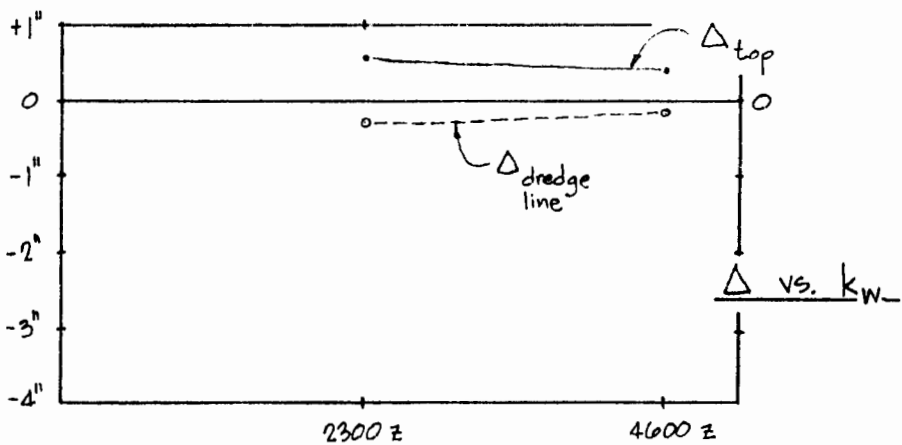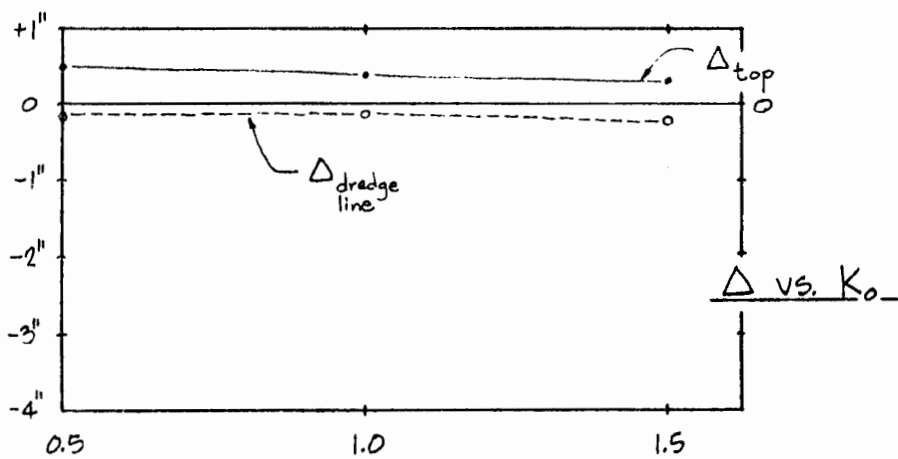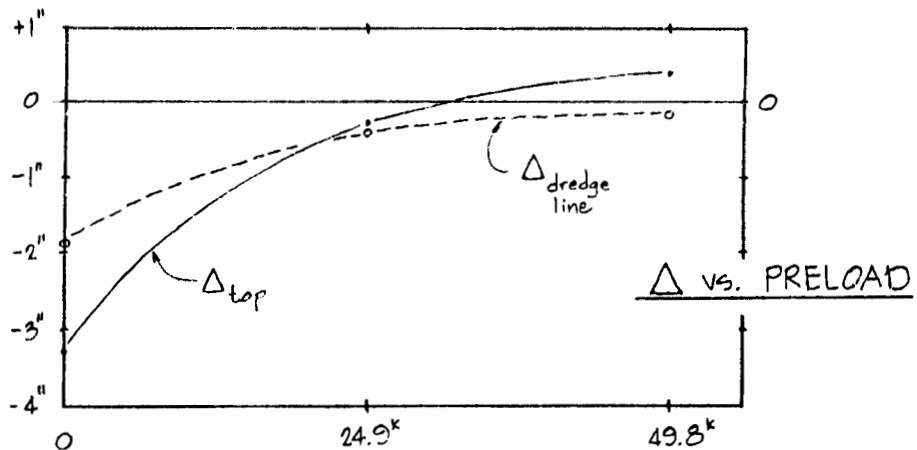
Figure 18. Deflection vs. Preload, K_O, and k_W.
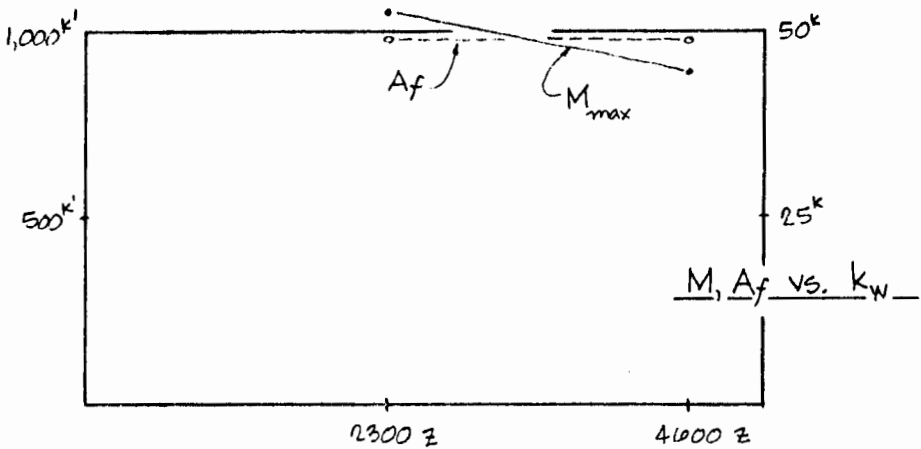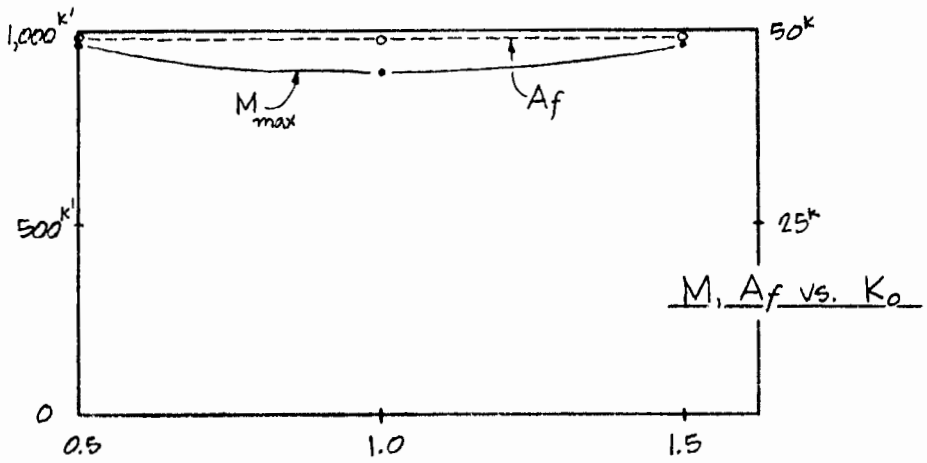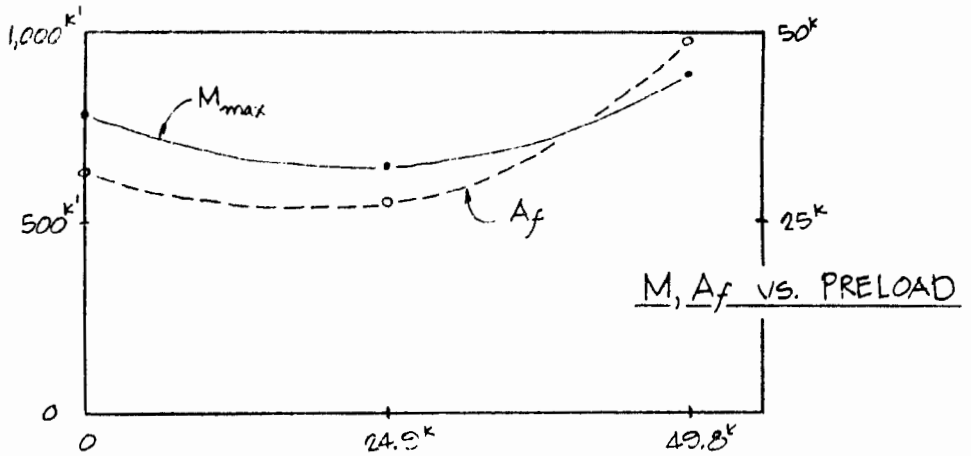
Figure 19. Moment and A_f vs. Preload, K_o, and k_w.
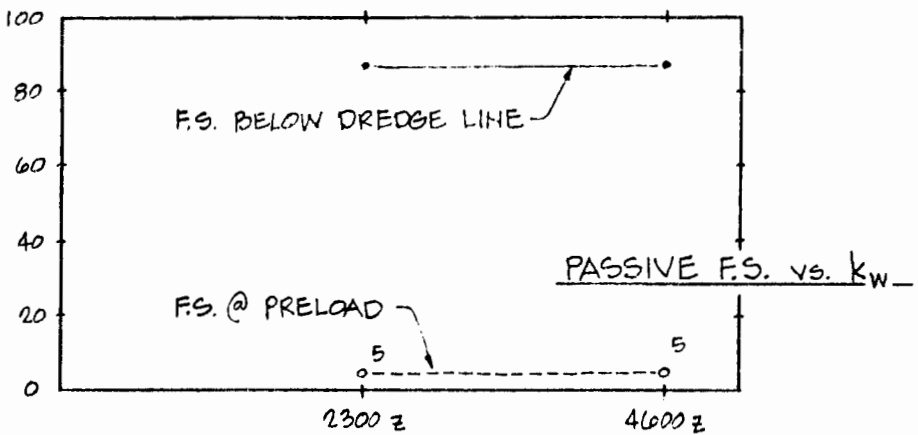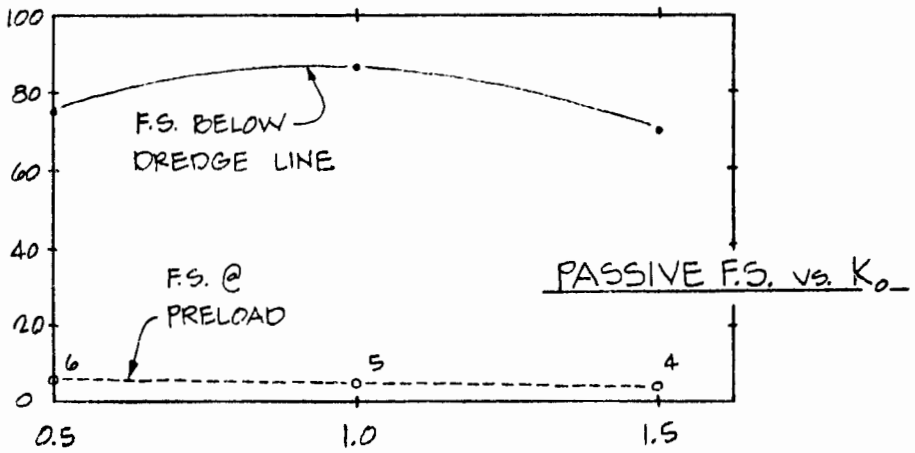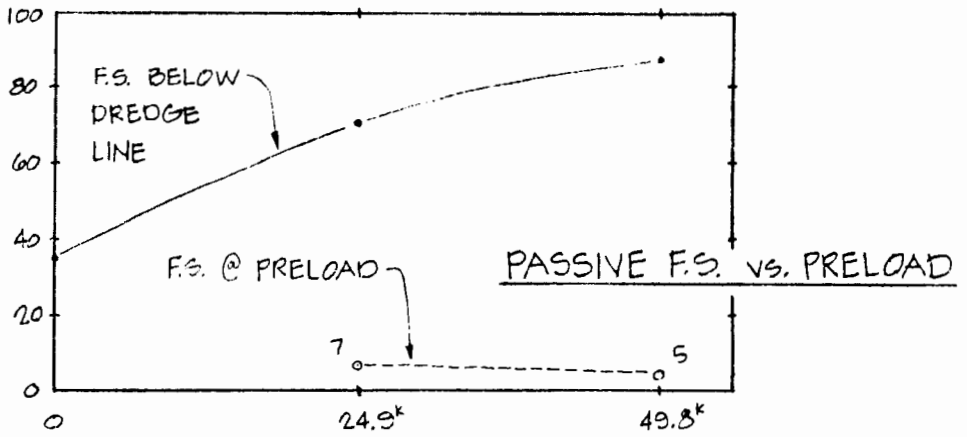
Figure 20. Passive F.S. vs. Preload, K_O, and k_W.

CHAPTER V

CONCLUSIONS AND RECOMMENDATIONS

PARAMETRIC STUDY CONCLUSIONS

Based on the parametric study consisting of 8
separate analyses of the BDW, as summarized in the
preceding section, several conclusions can be drawn. In
itemizing these conclusions, it is helpful in visualizing
the soil-structure response to separate the list into items
that result from variations in the 1) Structural
Conditions, from those that result from variations in the
2) Geotechnical Conditions.

Variations in the Structural Conditions

"Structural Conditions" are defined as variations in
anchor load, and anchor and wall stiffness.

1)   Preloading, to the full 49.8 kips/ft, reduces final
     dredge-line deflection from almost 2-inches to less
     than 1/4-inch outward.

2)   Preloading reduces final top of wall deflection from
     more than 3-inches outward to about 1/2-inch inward.

3)   Preloading increases final maximum bending moment by
     15-percent.

4) Preloading increases final anchor load 50-percent over the 0-preload case.

5) The amount of preload obtained is much more significant than variations in the axial stiffness of the anchors.

6) The maximum moments obtained were on the order of 1/2 to 2/3 of the wall cracking moment.

7) If the wall section is cracked, the change in maximum moment is small, but deflections are roughly doubled.

Variations in the Geotechnical Conditions

These conditions are defined as those whose variations create changes in the wall W-Y curve generation.

1) Safety Factor against passive soil failure behind the anchor during preloading is on the order of 5.

2) Final safety factor against passive failure below dredge line in front of the wall is 40 or more.

3) Variations in K_o, the in-situ at-rest pressure coefficient, have a negligible effect on deflections, anchor load, bending moment, and passive F.S.

4) Variations in K_w, the horizontal modulus, have a negligible effect on deflections, passive F.S., and anchor load.

5) Halving K_w results in a 20-percent increase in bending moment.

RECOMMENDED ANALYSIS PROCEDURE

The correct determination of retaining wall deflections, pressures, and bending moments is a soil-structure interaction problem. Currently, the most efficient solution is an application of the finite-difference method on the personal computer, using a non-linear code such as the BMCOL7-PC program (32). In utilizing BMCOL7, the designer must correctly address staged construction, anchor preload, wall cracking, and soil W-Y curve development.

Staged Construction for a Preloaded Anchor

The W-Y curve at any point on a retaining wall depends on the properties of the soil in contact with each side of the wall, as well as pre-existing vertical and horizontal stresses in the soil. Pre-existing vertical stresses depend upon soil overburden plus surcharge loads, and pre-existing horizontal stresses depend on the at-rest coefficient plus the effect of anchor preload from preceding runs.

When a tieback anchor is preloaded prior to wall excavation, the W-Y curves that act in response to the final excavation are different from those that act in response to the preload. Therefore at least 2 runs must be made on BMCOL7: one at preload, and a second at final excavation. An additional run would likewise be required

for every additional anchor down the vertical face of the wall.

The W-Y curves must be re-established at all locations for the second stage, including re-adjusting the displacement origin of the curves to account for the response at preload. Final deflections will consist of superimposing the result from the 2 runs.

It is normally not necessary to make additional runs, corresponding to multiple levels of excavation between preloaded anchors, provided that the soil pressures resulting from preload do not reach passive failure (i.e., the flat part of the W-Y curve). This is only likely to occur for weak soils, very high preloads, and/or very flexible walls.

The tieback anchor should be modeled as a concentrated load for the preload stage, and as a concentrated W-Y curve with the Y-origin displaced to correspond to the preload amount at the excavation stage.

Wall Cracking and Stiffness

The results of the present study indicate that wall cracking has a siginificant effect on final deflections. It is therefore recommended that wall cracking moment be calculated (normally it will be different for positive and negative moment), and compared with the resulting moments from each run. Where the cracking moment is approached or

exceeded, it will be necessary to make a re-run, entering
the cracked (transformed area) section stiffness for the
portion of the wall that is cracked. Since this may result
in a change in the length of the wall where moments exceed
Mcr, several iterations may be required for convergence,
for each run.

W-Y Curve Derivation

BMCOL7 requires that the soil load-deflection
response be described down the heighth of the wall. The
recommended procedure for establishing the W-Y curves is as
follows:

1) Determine the insitu effective vertical stress on
   each side of the wall, from any convenient theory.

2) Using classical theory and Eqs. 5 & 6, determine the
   active and passive pressure coefficients, K_a & K_p.

3) Determine the active and passive limits on each side
   of the wall from Eqs. 3 and 4.

4) Determine the W-axis intercept as the difference
   between Eqs. 2 from each side of the wall.

5) From pressuremeter test results, determine the linear
   increase in the pressuremeter modulus with depth,
   i.e., E_m/z.

6) Find the horizontal wall modulus, k_w, from the
   pressuremeter modulus and Eqs. 23 or 25, and Fig. 6.

7) Determine the displacement (y value) from y=0 to the

active and passive limits, by solving Eq. 7 for y,
taking W in Eq. 7 as the difference between the
active or passive limit and the net at-rest (W-axis)
intercept, as shown in Fig. 9.

RECOMMENDED AREAS FOR FURTHER STUDY

Based on the results of this study, the following
areas warrant further investigation:

1) Expand the BMCOL7-PC program to incorporate staged
   construction and preloaded anchors by automatically
   updating the W-y curves for succeeding stages and
   superposing the accumulated deflections from
   preceding stages.

2) Conduct Finite Element Method studies of the
   Permanent and Temporary Buttress Diaphragm Walls,
   using USACE's SOILSTRUCT program, to verify and
   refine the Finite Difference Method results and range
   of soil modulus values.

3) Conduct laboratory model studies to enhance the
   hyperbolic soil model input to SOILSTRUCT with
   pressuremeter test result data.

4) Make a pseudo 3-dimensional FEM study of the
   diaphragm walls, to identify important limitations of
   the Finite Difference Method analyses.

5) Research thoroughly the topic of large slurry wall

designs and case histories, emphasizing 3-D and field construction aspects and their effect on modeling with the Finite Element Method.

6) Study the existing ground horizontal stresses at the diaphragm wall site, and examine the impact on slope stability of the lock construction, using the FEADAM program (available at PSU).

7) Select appropriate soil/structure monitoring equipment to install at the Diaphragm Walls to monitor actual field deflections during and after construction.

REFERENCES

1. Baguelin, F., Frank, R., and Said, Y.H., "Theoretical Study of Lateral Reaction Mechanism of Piles," Geotechnique, Vol. 27, No. 3, 1977, pp. 405-434.

2. Baguelin, F., Jezequel, J.F., and Shields, D.H., The Pressuremeter and Foundation Engineering, Trans Tech Publications, Clausthal, Germany, 1978.

3. Briaud, J.-L., "Pressuremeter and Foundation Design," Specialty Conference on Use of In-Situ Tests in Geotechnical Engineering, ASCE, June, 1986.

4. Briaud, J.-L., Tucker, L.M., and Makarim, C.A., "Pressuremeter Standard and Pressuremeter Parameters,"The Pressuremeter and It's Marine Applications: Second International Symposium,ASTM STP 950, May 1986, pp. 303-323.

5. Briaud, J.-L., Smith, T., and Meyer, B., "Laterally Loaded Piles and the Pressuremeter: Comparison of Existing Methods," Laterally Loaded Deep Foundations: Analysis and Performance, ASTM STP 835, 1984, pp. 97-111.

6. Cornforth Consultants, Inc., Geotechnical Study: Exploration, Sampling, and Testing for Retaining Wall Parameters, New Bonneville Navigation Lock, U.S. Army Corps of Engineers, Portland District, October 1986.

7. Dawkins, W.P., Users Guide: Computer Program for Analysis of Beam-Column Structures with Nonlinear Supports (CBEAMC), U.S. Army Engineer Waterways Experiment Station, Vicksburg, Miss., June 1982.

8. Douglas, D.J., and Davis, E.H., "The Movement of Buried Footings Due to Moment and Horizontal Load and the Movement of Anchor Plates," Geotechnique, Vol. XIV, No. 2, June 1964, pp. 115-132.

9. Felio, G.Y., and Briaud, J.-L., "Conventional Parameters from Pressuremeter Test Data: Review of Existing Methods," The Pressuremeter and It's Marine Applications, Second International Symposium, ASTM STP 950, 1986, pp. 265-282.

10. Gleser, S.M., "Lateral Load Tests on Vertical Fixed-Head and Free-Head Piles," <u>Symposium</u> <u>on</u> <u>Lateral</u> <u>Load</u> <u>Tests</u> <u>on</u> <u>Piles</u>, ASTM STP No. 154, July 1953, pp. 75-101.

11. Gould, J.P., "Lateral Pressures on Rigid Permanent Structures," <u>Lateral</u> <u>Stresses</u> <u>in</u> <u>the</u> <u>Ground</u> <u>and</u> <u>Design</u> <u>of</u> <u>Earth</u> <u>Retaining</u> <u>Structures</u>, ASCE SMFD Specialty Conference Proceedings, June 1970, pp. 219-269.

12. Grant, W.P., and Hughes, M.O., "Pressuremeter Tests and Shoring Wall Design," <u>Use</u> <u>of</u> <u>In</u> <u>Situ</u> <u>Tests</u> <u>in</u> <u>Geotechnical</u> <u>Engineering</u>, Geotechnical SP No. 6, ASCE, June 1986, pp. 588-601.

13. Hajnal, I., Marton, J., and Regele, Z., <u>Construction</u> <u>of</u> <u>Diaphragm</u> <u>Walls</u>, John Wiley and Sons, 1984.

14. Hetenyi, M., <u>Beams</u> <u>on</u> <u>Elastic</u> <u>Foundations</u>, University of Michigan Press, Ann Arbor, Mich., 1946.

15. Haliburton, T.A., "Numerical Analysis of Flexible Retaining Structures," <u>Journal</u> <u>of</u> <u>the</u> <u>Soil</u> <u>Mechanics</u> <u>and</u> <u>Foundations</u> <u>Division</u>, ASCE SM6, Nov. 1968, pp.　1233-1251.

16. Haliburton, T.A., "Soil-Structure Interaction: Numerical Analysis of Beams and Beam-Columns, "<u>Technical</u> <u>Publication</u> <u>No.</u> <u>14</u>, School of Civil Engineering, Oklahoma State University, Stillwater, Oklahoma, September 1979.

17. Hunt, R.E., <u>Geotechnical</u> <u>Engineering</u> <u>Analysis</u> <u>and</u> <u>Evaluation</u>, McGraw-Hill Book Company, 1986, pp. 171-187.

18. Huntington, W.C., <u>Earth</u> <u>Pressures</u> <u>and</u> <u>Retaining</u> <u>Walls</u>, John Wiley and Sons, 1957.

19. Lukas, R.G., and LeClerc de Bussy, B., "Pressuremeter and Laboratory Test Correlations for Clays," <u>Journal</u> <u>of</u> <u>the</u> <u>Geotechnical</u> <u>Engineering</u> <u>Division</u>, ASCE, GT9, Sept., 1976, pp. 945-962.

20. Matlock, H., and Reese, L.C., "Generalized Solution for Laterally Loaded Piles," <u>Journal</u> <u>of</u> <u>the</u> <u>Soil</u> <u>Mechanics</u> <u>Division</u>, ASCE, Vol. 86, No. SM5, October 1961, pp. 673-694.

21. Matlock, H., and Ingram, W.B., "Bending and Buckling of Soil-Supported Structural Elements," A Paper Presented to the 2nd Pan-Am Conference, SMFE, Brazil, 1963.

22. McClelland, B., and Focht, J.A., Jr., "Soil Modulus for Laterally Loaded Piles," Journal of the Soil Mechanics and Foundations Division, ASCE Vol. 82, No. SM4, October 1956, pp. 1-22.

23. NAVFACS, Design Manual 7.1, Soil Mechanics, Department of the Navy, Naval Facilities Engineering Command, Alexandria, Virginia, 1982.

24. NAVFACS, Design Manual 7.2, Foundations and Earth Structures, Ibid.

25. Poulos, H.G., and Davis, E.H., Elastic Solutions for Soil and Rock Mechanics, John Wiley and Sons, New York, 1974.

26. Reese, L.C., and Desai, C.S., Chapter 9, Numerical Methods in Geotechnical Engineering, McGraw-Hill Book Company, New York, 1977.

27. Robinson, K.E., "Horizontal Subgrade Reaction Estimated from Lateral Loading Tests on Timber Piles," Behavior of Deep Foundations, ASTM STP 670, 1979, pp. 520-536.

28. Squier, L.R., and Associates, Phase II, Tieback Test Program, Bonneville Navigation Lock, U.S. Army Corps of Engineers, Portland District, November 1986.

29. Smith, T.D., "Pressuremeter Design Method for Single Piles Subjected to Static Lateral Load," Vol. I and II, a dissertation submitted to the graduate college of Texas A&M University in partial fulfillment of the requirements for Doctor of Philosophy, August 1983.

30. Smith, T.D., Pressuremeter Testing and Design Considerations for Upstream Temporary Diaphragm Wall, Buttress Diaphragm Wall, and Downstream Approach Walls, Bonneville Navigation Lock, Portland State University, Department of Civil Engineering, October 1985.

31. Smith, T.D., and Ray, B., "Shear Mobilization on Laterally Loaded Shafts," Geotechnical Aspects of Stiff and Hard Clays, Geotechnical SP No. 2, ASCE, April 1986, pp. 60-68.

32. Smith, T.D., BMCOL7, Soil-Foundation Interaction
    Program (Nonlinear Behavior), User's Manual, Portland
    State University, August 1984.

33. Smith, T.D., "Pile Horizontal Soil Modulus Values,"
    Journal of the Geotechnical Engineering Division, ASCE,
    September, 1987.

34. Sowers, G.F., Introductory Soil Mechanics and
    Foundations: Geotechnical Engineering, MacMillan
    Publishing Company, 4th Ed., 1979.

35. Terzaghi, K., "Evaluation of Coefficients of Subgrade
    Reaction," Geotechnique, Vol. V, No. 4, December 1955,
    pp. 297-326.

36. Terzaghi, K., Theoretical Soil Mechanics, John Wiley
    and Sons, New York, 1943.

37. U.S. Army Corps of Engineers, Geology, Excavation, and
    Foundation Design Memorandum No. 3, Bonneville
    Navigation Lock, USACE Portland District, January 1984.

38. Xanthakos, P.P., Slurry Walls, McGraw-Hill Book
    Company, 1979.

39. Birang, Farahnaz, "Soil Structure Interaction with
    Nonlinear P.C. Beam-Column Schemes," a research project
    report submitted to the Civil Engineering Department of
    Portland State University in partial fulfillment for
    the degree of Master of Science, 1987.

NOTATION AND ABBREVIATIONS

A_f Final (stage-2) Anchor force.

A_{ps} Area of prestressed tieback anchors.

BE   Best estimate configuration.

BDW   Buttress Diaphragm Wall.

BRI   Bonney Rock Intrusive.

c   Cohesion.

D   Pressuremeter probe diameter.

E_m Menard (pressuremeter) modulus.

EI_{cr} Cracked bending stiffness of wall.

EI_g Gross bending stiffness of wall.

EL   Elevation.

FDM   Finite difference method.

FEM   Finite Element method.

FS   Factor of safety.

$f'c$ Concrete strength.

f_{ps} Tieback anchor prestress level.

f_{pu} Tieback anchor ultimate strength.

G   Shear modulus.

GWL   Groundwater level.

H_w Heighth of wall.

LC   Loading condition.

l_h Terzaghi's material coefecient for subgrade reaction.

I_w Coefficent for walls from pressuremeter modulus.

K_a Coefficient of active earth pressure.

K_o Coefficient of insitu earth pressure at-rest.

K_p Coefficient of passive earth pressure.

k_h Terzaghi's horizontal modulus of subgrade reaction.

k_w Horizontal modulus of subgrade reaction for walls.

L   Pressuremeter probe length; unbonded tieback length.

M_{cr} Cracking moment.

M_{max} Maximum moment.

p   Horizontal pressure.

PC   Personal computer.

PMT   Pressuremeter.

PSU   Portland State University.

R   PMT cavity radius.

R_o Initial PMT cavity radius.

R_w Equivalent gage distance over which ϵ_w produces y.

RSD   Reworked slide debris.

SB   Slide block material.

SSI   Soil-structure interaction.

Tw   Tertiary Weigle Formation.

USACE U.S. Army Corps of Engineers.

V   PMT cavity volume.

V_m Average volume for a given PMT pressure change.

V_o Initial PMT cavity volume.

W   Horizontal wall line-load.

W_a Active soil line-load against wall.

W_o Horizontal wall line-load in at-rest condition.

W_p Passive soil line-load against wall.

y Horizontal displacement.

α Angle from vertical of wall back face.

β Angle above horizontal of sloping surcharge.

Δ Wall deflection.

∂ Angle of wall friction.

ϵ_r Radial strain.

ϵ_w Strain in soil immediately behind wall.

ϵ_Θ Tangential strain.

γ Soil unit weight.

ν Poisson's ratio.

ϕ Angle of internal friction.

σ_r Radial stress.

σ_v Vertical effective stress from all causes.

x Effective width of wall.

z Vertical depth.